Geothermics 95 (2021) 102120

Contents lists available at ScienceDirect

Geothermics

journal homepage: www.elsevier.com/locate/geothermics

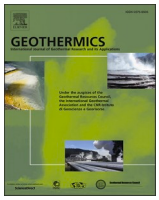

Geochemical investigations of the geothermal systems from the Island of Sicily (southern Italy)

Assunta Donato [1,*], Franco Tassi [2,3], Giovannella Pecoraino [4], Adele Manzella [1], Orlando Vaselli [2,3,5], Esterina Gagliano Candela [4], Alessandro Santilano [1], Leonardo La Pica [4], Claudio Scaletta [4], Francesco Capecchiacci [2]

[1] Institute of Geosciences and Earth Resources – CNR, Via G. Moruzzi 1, 56124 Pisa, Italy
[2] University of Florence, Department of Earth Sciences, Via La Pira 4, 50121 Florence, Italy
[3] Institute of Geosciences and Earth Resources – CNR, Via La Pira 4, 50121 Florence, Italy
[4] Istituto Nazionale di Geofisica e Vulcanologia – Sezione di Palermo, Via Ugo La Malfa, Palermo, Italy
[5] Istituto Nazionale di Geofisica e Vulcanologia – Sezione di Bologna, Via Franceschini, Bologna, Italy

ARTICLE INFO

Keywords:
Fluid geochemistry
Geothermal exploration
Stable isotopes
Dissolved gases
Tectonics

ABSTRACT

Sicily hosts many natural manifestations that include thermal waters, gas discharges and mud volcanoes. Due to the significant geodynamic and geological differences, the fluid discharges along a NE-WS–oriented transect that run from the Peloritani Mts. to the Sciacca Plain shows a large variability in water and gas chemical and isotopic compositions. The studied waters are characterized by Ca-HCO_3, Ca(Mg)-SO_4, Ca-Cl and Na-Cl compositions produced by distinct geochemical processes such as water-rock-gas interactions, mixing between deep and shallow aquifers and seawater and direct and reverse ion exchanges. The gas chemistry is dominated by CO_2 to the east and CO_2-N_2 to the west of the study area, whereas the central part shows mud volcanoes discharging CH_4-rich gases. Water isotopes suggest that the thermal waters are fed by a meteoric recharge, although isotopic exchange processes between thermal fluids and host rocks at temperature >150°C are recognized. Accordingly, liquid geothermometry suggests equilibrium temperatures up to 220°C. The carbon in CO_2 and helium isotopes of the emissions from the westernmost sector of Sicily indicate that these two gases consists of up to 40 % of a mantle component, the latter decreasing to the east down to 10% where CO_2 of thermometamorphic origin dominates. Accordingly, conceptual models of the fluid circulation for the western, central and eastern sectors are proposed. The regional geothermal reservoir, hosted in carbonates in the western sector and locally outcropping, is of low to medium temperature. Higher temperature conditions (up to 200-220°C) are suggested by geothermometry and probably related to deeper levels of the system. Sicily can be regarded as a potentially suitable area for future investigations to evaluate specific activities aimed at exploiting the geothermal resource.

1. Introduction

Sicily is the southernmost region of Italy and the largest island of the Mediterranean Sea and is located in a context of collisional regime at the border between the African and Eurasian plates. Setting aside the active volcanic arc of the Aeolian Islands and the lithospheric deep-tearing-related volcano of Etna (e.g. Aiuppa et al., 2000; Brusca et al., 2001; Doglioni et al., 2001), a relatively large variety of thermal manifestations at the surface occurs, such as thermo-mineral waters, diffuse soil degassing, bubbling pools and mud volcanoes, which are strictly depending on the complex regional geological-structural setting.

Fluid geochemistry applied to geothermal exploration is an excellent tool for depicting conceptual models of hydrothermal fluid circulation aimed at identifying: 1) heat source(s) (e.g. Caracausi et al., 2013; De Siena et al., 2017; Guo et al., 2017); 2) chemical-physical conditions and related chemical-physical processes controlling the fluid reservoir chemistry (e.g. Gianelli and Grassi, 2001; Benavente et al., 2016) and 3) water recharge (e.g. Cheng et al., 2010; Minissale and Vaselli, 2011).

Previous geochemical studies indicated a promising geothermal potential in several areas of the region (e.g. Carapezza, 1977; Alaimo et al., 1978; Camarda, 2004; Grassa et al., 2006; Italiano et al., 2006; Giammanco et al., 2008), although further investigations are needed to

* Corresponding Author
E-mail address: assunta.donato@igg.cnr.it (A. Donato).

https://doi.org/10.1016/j.geothermics.2021.102120
Received 21 December 2020; Received in revised form 7 April 2021; Accepted 12 April 2021

provide a reliable estimation of the resource.

This study presents and discusses the results of a geochemical survey carried out in 2015 and 2016 on the fluids discharged from the Sicily mainland, from a wide area extending in NE-SW direction from the Peloritani Mts. to the Sciacca area, through the Caltanissetta basin (Fig. 1). These geochemical data were integrated with those available in the literature.

The aims of this study were to: i) investigate the primary source(s) and physico-chemical processes controlling the chemical features of the thermal and cold springs in relation to the tectonic setting and ii) construct a conceptual model targeting the circulation paths and the main water-gas-rock interaction processes.

2. Regional framework and geological setting

Sicily belongs to the Apennine–Maghrebian chain that developed by the late Oligocene along the border of the African-European plate (Catalano et al., 1996). This segment of the chain links the African Maghrebids to the Southern Apennines, through the Calabrian-Peloritan Arc (Fig. 1). Different geodynamic environments and tectonic regimes concurred to the present geological architecture (Catalano & D'Argenio, 1982; Roure et al., 1990; Nigro and Renda, 1999; Bello et al., 2000; Catalano et al., 2000a; Accaino et al., 2011). The Sicilian Fold and Trust Belt (FTB) consists of an articulated chain-foredeep-foreland system. The foreland area emerges in southeastern Sicily and extends to the sea in the Sicily channel and Ionian Sea. The African foreland domain is mainly characterized by a sedimentary succession (about 7 km thick) of Meso-Cenozoic platform carbonates and Tertiary clastic deposits that lie above the crystalline basement. A narrow WNW-ESE-oriented Pliocene-Quaternary foredeep, is partially buried below the external sector of the chain in correspondence of the Gela Thrust System (Catalano et al., 2013). The FTB has a thickness of >15 km and occupies a large part of the island and the adjacent sea areas. The chain consists of three main elements (Catalano, 2004): i) "European"; 2) "Tethyan" and 3) "African". The "European" element outcrops in the northeastern part of Sicily, close to the Peloritani Mts., which are the Sicilian part of the Calabro-Peloritan Arc (Amodio Morelli et al., 1976). The "Tethyan" element is associated with the sedimentary succession named "Sicilides" (Ogniben, 1960). The latter consists of basin carbonates and pelitic-arenaceous deposits that detached from their substrate, Upper Jurassic to Lower Miocene in age. The "African" element is dominated by Mesozoic-Lower Miocene deep-sea carbonate and silicoclastic rocks (formed in the domains known as Imerese and Sicano) and Meso-Cenozoic carbonate rocks deposited in the domains known as Pre-Panormide, Panormide, Trapanese, Saccense and Ibleo-Pelagiana Carbonate Platforms (Catalano & D'Argenio, 1978, 1982).

The tectonic setting of the collisional complex shows significant differences in various sectors of the island. Active tectonics, with different regimes, is still occurring. In historical times, Sicily has experienced intense seismicity, catastrophic events (e.g. Gasparini et al., 1982; Anderson & Jackson, 1987; Monaco et al., 1996; Giammanco et al., 2008) and volcanic activity (e.g. Peccerillo, 2017 and references therein). Carminati and Doglioni (2012) and Carafa & Barba (2013) identified on a regional scale two macro tectonic regimes in the island: 1) the peri-Tyrrhenian area, characterized by an extensive regime closely related to the opening of the south-Tyrrhenian retro-arc basin and 2) a compressional zone in central and southern Sicily, linked to the continental collision processes along the European-African margin.

The western sector of the island has a high heat flow (up to 100 mW/m^2), whereas it is lower in the central-northern sector of the island, between the Nebrodi and the Madonie Mts. (from 50 to 70 mW/m^2). Heat flow values up to 150 mW/m^2 and 200 mW/m^2 are shown in the Sicilian Channel and in the Aeolian Archipelago, respectively. Heat flow values up to 80 mW/m^2 also characterize the southeastern area of the island (Iblea portion). Sicily mainland hosts a regional hydrothermal reservoir in carbonate rocks (Montanari et al., 2014, 2017).

Geologically, the study area (Fig. 1) can be divided into 3 main sectors, as follows.

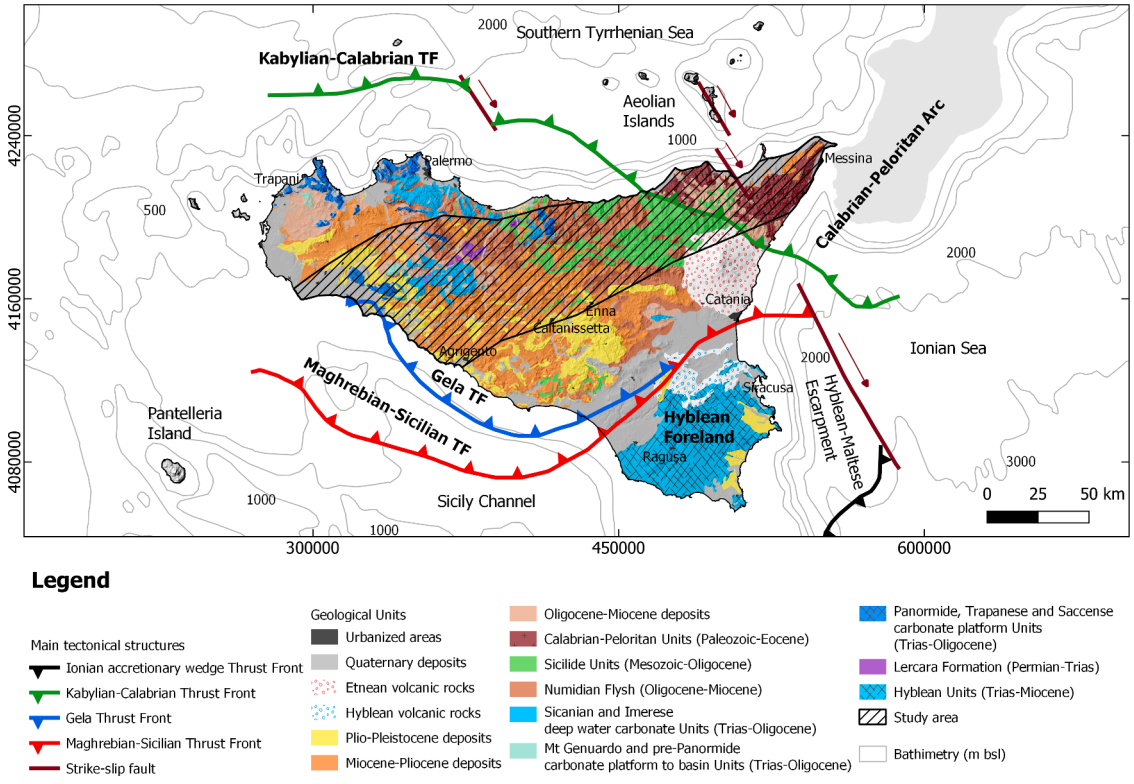

Figure 1. Geological-structural map of Sicily (modified from Trumpy et al., 2015).

2.1. Eastern sector: Peloritani Mts.

From a structural point of view, the Peloritan units belong to the European element and represent the geometrically highest sector of the Sicilian chain (Fig. 1). The Calabro-Peloritan Arc is made up of layers of Hercynian crystalline basement, including fragments of the original Meso-Cenozoic coverage.

2.2. Central sector: Nebrodi Mts., Madonie Mts. and Caltanissetta Basin

Towards the west, in proximity of the Nebrodi Mts., the Sicilides Units overlie the carbonate Panormide Units and the Numidian Flysch (Fig. 1). Near the Madonie Mts., the tectonic building is characterized by the occurrence of the deep-sea Imerese Units. In the central part of the study area, a thick morpho-structural depression (the "Caltanissetta Basin") occurs. During the progressive Neogene-Quaternary overlapping of the tectonic layers towards the south, several syntectonic basins developed above the wedge (Butler & Grasso, 1993; Butler et al., 1995). The filling sequence is constituted by marls, clays, sandstones and Messinian evaporitic successions.

2.3. Western sector: Sicani Mts. and Sciacca Basin

The tectonic setting from the Sicani Mts. to the Sciacca basin includes three structural levels (Catalano et al., 2013): a) the lower level is a tectonic wedge up to 9 km of imbricated units with >3 km thick platform carbonates belonging to the Panormide, Trapanese and Saccense domains; b) the intermediate structural level consists of basin carbonates from the Imeresi (to the north) and Sicani (to the south) domains, about 2-3 km thick (these units overlap the imbricated units of the carbonate platform); c) the upper level is represented by: i) Miocene molasse deposits, Messinian evaporites and Lower Pliocene limestones and ii) Middle Pliocene-Lower Pleistocene clastic-carbonate deposits (Fig. 1).

2.4. Territory and climate

Sicily is characterized by a very articulated orography, mostly hilly (about 61%) with mountain complexes that represent about 24% of the entire territory. The orography shows marked distinctions between the northern portion predominantly mountainous, the central-southern and south-western portions essentially hilly, a plateau in the southeastern portion and Etna volcano (>3300 m abs) in eastern Sicily. The harshest orographic area is concentrated mainly on the Tyrrhenian Sea side, where the northern chain includes the Peloritani Mts. and the Nebrodi Mts. complex. In the central and western sector, the mountain groups of the Madonie Mts., the Trabia Mts., the Palermo Mts., the Trapani Mts. and, more inland, the Sicani Mts. group develop. The eastern sector of Sicily hosts the volcanic complex of Mount Etna and the Hyblean plateau. The torrential rivers are numerous and many of them are short and rapid. The most important rivers in terms of the abundance of perennial water flow on the eastern side are, as follows: Simeto, Dittaino, Gornalunga and Alcantara. According to the mean temperature and rainfall (Fig. 2), Sicily is characterized by a typical Mediterranean climate. The average temperature in the hottest months (July to September) is > 22°C whilst the meteoric precipitations are mostly concentrated in the coldest periods (autumn-winter). Due to the morphological complexity of the island, there are remarkable differences in the thermo-pluviometric regimes as they vary from subtropical temperate to warm temperate and sublittoral temperate, subcontinental temperate, cool temperate with the average annual temperature ranging from 11 to 20°C. The total annual rainfall is comprised between 385 mm, in the district of Caltanissetta, to 1192 mm on the slopes of Etna volcano (Drago, 2005).

3. Sampling and analytical methods

3.1. Water and gas sampling

Waters and associated dissolved and bubbling gases from wells (w), springs (s), drainage tunnels (dt), mud volcanoes (mv) and bubbling pools (bp) were collected from 65 sites during six sampling campaigns carried out between March 2015 and June 2016. The sampling sites were distributed in a relatively wide area (about 12,000 km^2) extending from the Peloritani Mts. (NE) to the Sciacca Basin (WSW) (Fig. 3).

Chemical-physical parameters of waters (pH, Eh, temperature and electrical conductivity) were measured *in situ*. Four aliquots of water were collected in polyethylene bottles, as follows: i) 125 mL, filtered at 0.45 μm for the analysis of anions and NH_4^+; ii) 50 mL, filtered at 0.45 μm and acidified with HCl for the analysis of the main cations; iii) 50 mL of "as it is" water for the analysis of the δD and $\delta^{18}O$ of H_2O.

The dissolved gases were collected in pre-evacuated 250 mL glass flasks tapped with Teflon stopcocks according to the method described by Tassi et al. (2008). Gas samples from bubbling pools and mud volcanoes were collected using an overturned plastic funnel positioned above the emission point and connected via silicone tubes to glass flasks consisting of 1) Giggenbach-type bottles and 2) pyrex flasks equipped with two thorion valves.

3.2. Chemical and isotopic analysis of waters

At each site, outlet temperature, electrical conductivity, pH and Eh were measured in-situ with a Thermo Orion 3 Star conductivity meter and thermometer, a Thermo Orion 3 Star pH-meter, and a Thermo Orion model 250, respectively. Bicarbonates were determined within 24h after

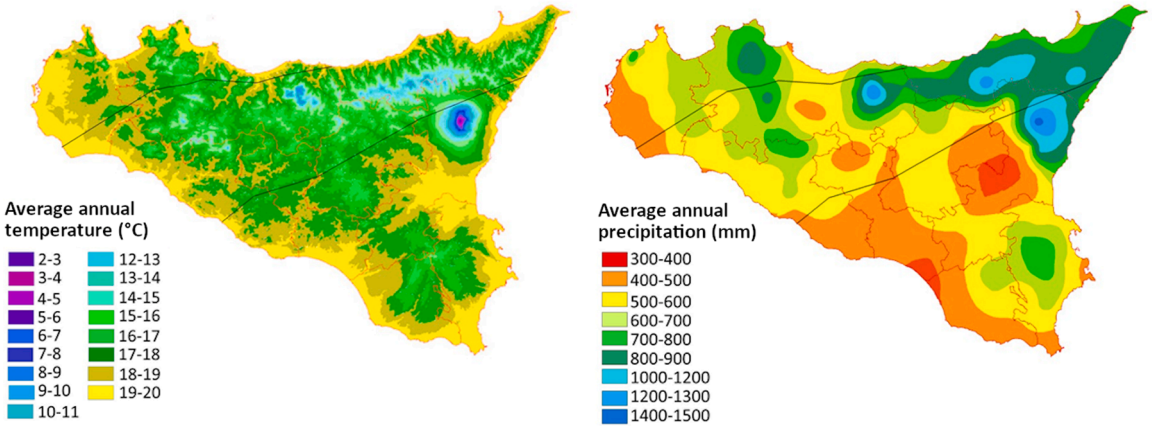

Figure 2. Maps of average annual precipitation (in mm, on the right) and temperature (°C, on the left). (Drago, 2005 modified).

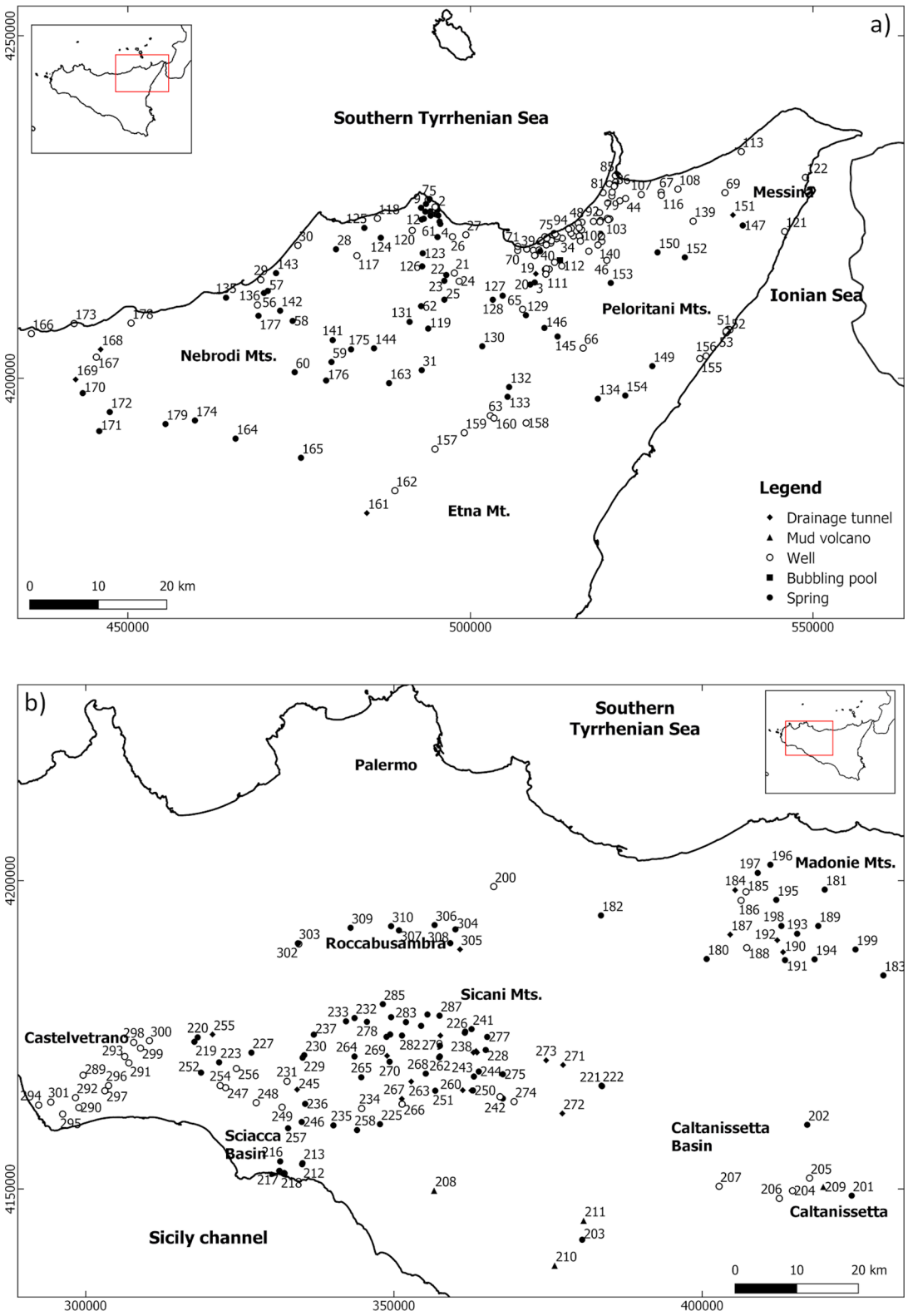

Figure 3. Location of the original and literature sampling sites (Site references in Tabs. 1 and 2 in supplementary material)

sampling in the laboratory by acidimetric titration with 0.01N HCl and methyl-orange as indicator. Anions and cations were analyzed at the Department of Earth Sciences of Florence (Italy) by ion chromatography (IC) using a Metrohm 761 and Metrohm 861, respectively. The analytical error of AC and IC was <3%. The $^{18}O/^{16}O$ and $^{2}H/^{1}H$ isotopic ratios (expressed as $\delta^{18}O$ and $\delta^{2}H$ ‰ vs. V-SMOW, respectively) were simultaneously measured by laser spectroscopy using a Liquid Water Isotope Analyser from Los Gatos Research at the Fluid Geochemistry Laboratory of CNR-IGG of Pisa (Italy). The analytical accuracy was ±0.2 ‰ for $\delta^{18}O$ and ±1 ‰ for δD. The 2004-2005 water samples (Regione Siciliana, Piano di Tutela delle Acque della Regione Sicilia, 2006) were collected and stored in low-density polyethylene flask. Samples were

analyzed in the laboratories of the Istituto Nazionale di Geofisica e Vulcanologia (INGV), Sezione di Palermo (Italy). The main solutes were analyzed by using a ion chromatograph DIONEX DX 120, on separate unfiltered and unacidified (F^-, Cl^-, NO_3^-, SO_4^{2-}) and filtered (0.45μm), acidified (Na^+, K^+, Mg^{2+} and Ca^{2+}) sample aliquots (analytical precision ±3%). Dionex CS-12A and Dionex AS14A columns were used for the determination of cations and anions, respectively. The $^{18}O/^{16}O$ and $^{2}H/^{1}H$ isotopic ratios were analyzed by using Analytical Precision AP 2003 and FinniganMAT Delta Plus spectrometers respectively. The isotope ratios are expressed as the deviation per mil (δ‰) from the reference VSMOW. The analytical accuracy was ±0.1‰ for $\delta^{18}O$ and ±1‰ for δD. The saturation indices and the pCO_2 values ($\log pCO_2$) were computed using the PHREEQC speciation program (Parkhurst and Appelo, 1999).

3.3. Chemical and isotopic analysis of gases

The dissolved inorganic gases in the headspace of the sampling flasks (CO_2, N_2, Ar, O_2, and Ne) were measured by gas chromatography (GC) at the Department of Earth Sciences of Florence (Italy) with a Shimadzu 15A equipped with a Thermal Conductivity Detector system. CH_4 in low concentrations was analyzed using a Shimadzu 14A equipped with a Flame Ionization Detector system. The gas species in the liquid phase of the sampling flasks were recalculated according to the Henry's Law constants (Tassi et al., 2009). The analytical error for GC was ≤5%. The CO_2 from the gas phase in the headspace was used to determine the $^{13}C/^{12}C$ isotopic ratios (expressed as $\delta^{13}C$‰ V-PDB) with a Finnigan MAT 252 mass spectrometer at the Laboratory of Isotope Chemistry of the CNR-IGG in Pisa, after extraction and purification procedures by cryogenic traps (Vaselli et al., 2006). The free gases collected were analyzed at the laboratories of the Istituto Nazionale di Geofisica e Vulcanologia (INGV), Sezione di Palermo (Italy). The gaseous species were determined by a gas chromatograph (Clarus 500, Perkin Elmer) equipped with Column Carboxen 1000 and two detectors: Hot Wire Detector and Flame Ionization Detector. The analytical error was <3%. Helium, Neon, and the respective isotopic composition were only determined in the free gases. The gas mixture was purified in a stainless-steel preparation line and He and Ne were cryogenically separated at 42 and 82 K, respectively. The $^{3}He/^{4}He$ ratio and $^{4}He/^{20}Ne$ isotopic ratios were determined using a Helix SFT-GVI mass spectrometer, following the internal protocol reported in Rizzo et al. (2015). The analytical uncertainty in the determination of elementary He and Ne concentrations was <5%. The $^{3}He/^{4}He$ ratios was corrected for air contamination based on the $^{4}He/^{20}Ne$ ratios (Giggenbach et al., 1993), and expressed as R/Ra (where R is the $^{3}He/^{4}He$ ratio measured in the sample and Ra is the $^{3}He/^{4}He$ ratio in air, whose value is 1.39×10^{-6}). The analytical error was <0.3%. The isotopic composition of CO_2, expressed as $\delta^{13}C\text{-}CO_2$ vs. PDB, was determined by a dual-inlet mass spectrometer (Finnigan Delta Plus) after applying standard purification procedures to the gas samples. The analytical error was <0.2%.

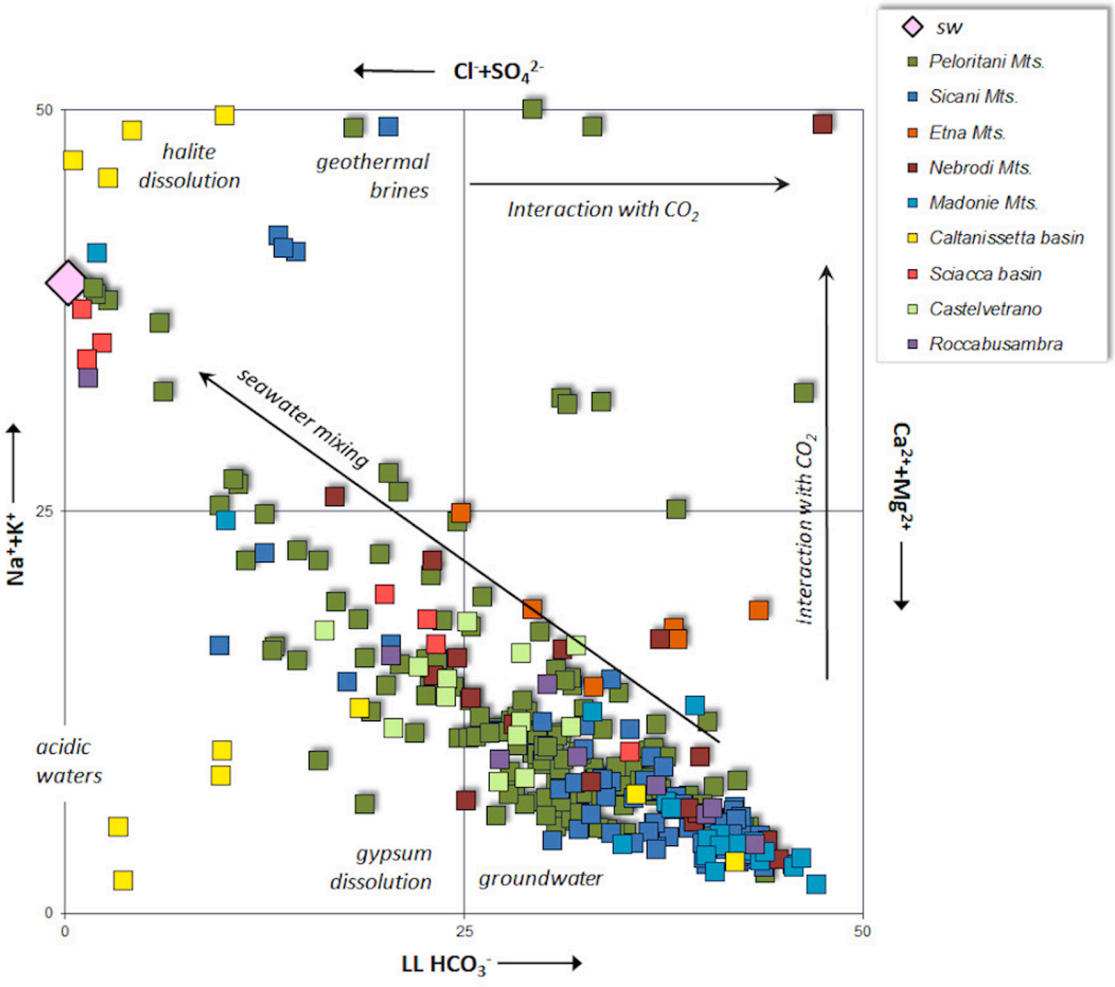

Figure 4. Langelier–Ludwig diagram for the investigated water samples (Data references in Table 1 in supplementary material).

4. Results

4.1. Water geochemistry

The chemical composition of cold and thermal waters is given in Table 1 in supplementary material. The outlet temperatures ranged from 7.9°C (#31) to 54.8°C (#214) while the pH varied from slightly acidic (5.61: #214) to strongly basic (9.45: #25). The TDS values were comprised between 36 (#199) and 40,904 (#52) mg/L. Eventually, the Eh values were varying from -398 mV (#208) to 602 mV (#181).

The Langelier-Ludwig diagram (Langelier & Ludwig, 1942) shows a significant compositional variability (Fig. 4) as also indicated by the anionic (e.g. Giggenbach, 1991) and cationic (e.g. Giggenbach et al., 1983) ternary diagrams (Fig. 5). Accordingly, the studied waters can be grouped, as follows:

Ca(Mg)-HCO_3 waters – Most of cold waters are Ca(Mg)-HCO_3, with a pH from weakly acid to alkaline (6.13 - 9.45) and TDS from 51 to 1,388 mg/L. The Eh is almost always positive except for a few samples from the Peloritani Mts. (#71) and the Castelvetrano Plain (#298 and #300) where is negative. The Ca^{2+}/Mg^{2+} ratios are mainly >1 although it is <1 for a number of waters from the Peloritani Mts. (#94, #78, #9, #10, #111, #138 and #66), Nebrodi Mts. (#167), Etna Mt. (#162 and #158), Sicani Mts. (#248 and #247) and Castelvetrano Plain (#298). Temperatures up to 31°C were recorded for #48, #50, #212, #213, #200, #216, #303 whose pH was from 6.13 to 8.03 and TDS up to 1,150 mg/L (with the exception of #50 in the eastern sector of Peloritani Mts. with TDS = 2,300 mg/L).

Na-HCO_3 waters – This group includes the cold waters from the Peloritani Mts. (#136, #23, #24, #38, #45 and #36), Etna Mt. (#161) and Nebrodi Mts. (#163), with pH from neutral to alkaline, TDS up to 1,950 mg/L and positive Eh values with the exception of #38 (-257 mV). Three thermal (temperature up to 30.2°C) waters from the Peloritani Mts. (#21, #42 and #32) belong to this group with variable pH, TDS and Eh values: from 6.71 to 7.9, from 408 to 6,000 mg/L and from -309 to +67 mV, respectively. Two thermal waters from the Peloritani Mts. (#55) and Sciacca basin (#218) have intermediate Na(Ca)-$HCO_3(SO_4)$ character.

Na-Cl waters – These waters are characterized by pH from 5.6 to 7.93, highly variable TDS values (from 36 to 40,904 mg/L), and negative Eh with the exception of #14, #8, #16, #155, #172, #6, #147 and #5 (Peloritani Mts.) and #199 (Madonie Mts.). Most Na-Cl waters from the Peloritani Mts. (#49, #51, #52, #53), Sicani Mts. (#219, #221, #222, #223), Sciacca Basin (#217, #215, #214) and Madonie Mts. (#180) have relatively high temperatures (up to 54.8°C; #214). Mud volcanoes (Caltanissetta Basin: #208, #209, #210, #211) are also Na-Cl. Two waters (#126: Peloritani Mts.) and (#225: Sicani Mts.) show a Na-Cl (HCO_3) composition.

Na-SO_4 (HCO_3) waters – Within this group there are only three waters, with pH between 6.5 and 9.02 and reducing (#26 and #27: Peloritani Mts.) to oxidizing (#172: Nebrodi Mts.) conditions.

Ca-Cl waters – Four water samples (#54 and #122: Peloritani Mts., #252: Sicani Mts. and #289: Castelvetrano Basin) fall within this group with temperature ranging from 18.1 to 21.4, pH from 7.1 to 8.5, positive Eh, except #122 (-45 mV) and TDS between 913 and 1,200 mg/L.

Ca(Mg)-SO_4 waters – The Ca/Mg ratio >1 was related to #82 and #148 (Peloritani Mts.) and #204, #206, #207, #201 and #203 (Caltanissetta Basin) whereas Mg was enriched with respect to Ca in #151, #113 and #7 (Peloritani Mts.). Intermediate compositions were recorded for #220 (Sicani Mts.: Ca(Mg)-SO_4(Cl)) and #39 (Peloritani Mts.: Ca-$SO_4(HCO_3)$) with temperatures of 39.2 and 21.3°C, respectively.

4.2. Water isotopes

The $\delta^{18}O$-H_2O and $\delta^{2}H$-H_2O values ranged from -9.3 to +12.7‰ and from -57.0 to 0.1‰ *vs. V-SMOW*, respectively (Table 1 in supplementary material). Most $\delta^{18}O$-H_2O and $\delta^{2}H$-H_2O values plot along the *Sicilian Meteoric Water Line* (SMWL; Liotta et al., 2013) (Fig. 6). Few samples, i.e. #208 and #209 (Caltanissetta Basin), #214 (Sciacca Basin), #53 and #52 (Peloritani Mts.) were enriched in both ^{18}O and ^{2}H with respect to the local meteoric recharge. Samples #215 (Sciacca Basin), #51 (Peloritani Mts.), #221, #222, #223 (Sicani Mts.) and #180 (Madonie Mts.) only showed ^{18}O enrichments. The #131 sample (Peloritani Mts.) represents an unexpected outlier in the isotopic composition of oxygen. The negative shift of ^{18}O may be reflecting the isotopic exchange between water and CO_2, according to the reaction (1):

$$0.5C^{16}O_2 + H_2\,{}^{18}O \rightarrow 0.5C^{18}O_2 + H_2^{16}O \quad (1)$$

which determines an increase in ^{18}O of CO_2 and consequent enrichment of ^{16}O of the aqueous phase (e.g. Chiodini et al., 2000). It is to mention that such isotopic signature can mark the contribution by fossil brines. However, the chemical composition of #131 is similar to that of the surrounding springs. Consequently, the $\delta^{18}O$-H_2O value may be affected an analytical error.

4.3. Chemical and isotopic compositions of dissolved and bubbling gases

Gas species were determined from 68 sites. The concentrations of the dissolved gases and bubbling gases (in % by vol.) from mud volcanoes and pools are listed in Table 2 in supplementary material. CO_2 was largely the most abundant gas compound (up to 99.6% by vol.) in the Peloritani Mts. and progressively decreased towards NW (Palermo and Madonie Mts.) and SW (Sicani Mts., Sciacca Basin), where a significant

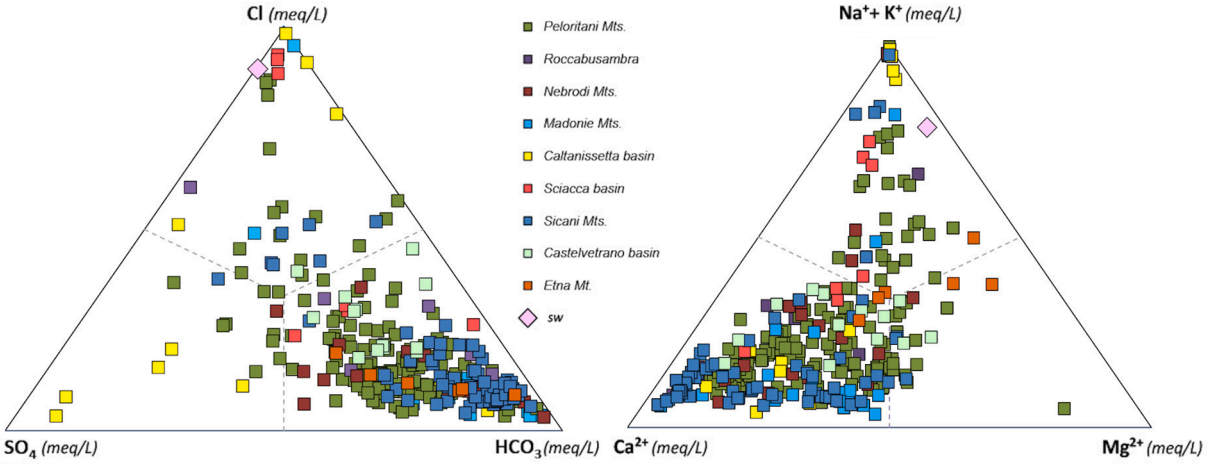

Figure 5. Ternary diagrams of the anionic and cationic species (Data references in Table 1 in supplementary material).

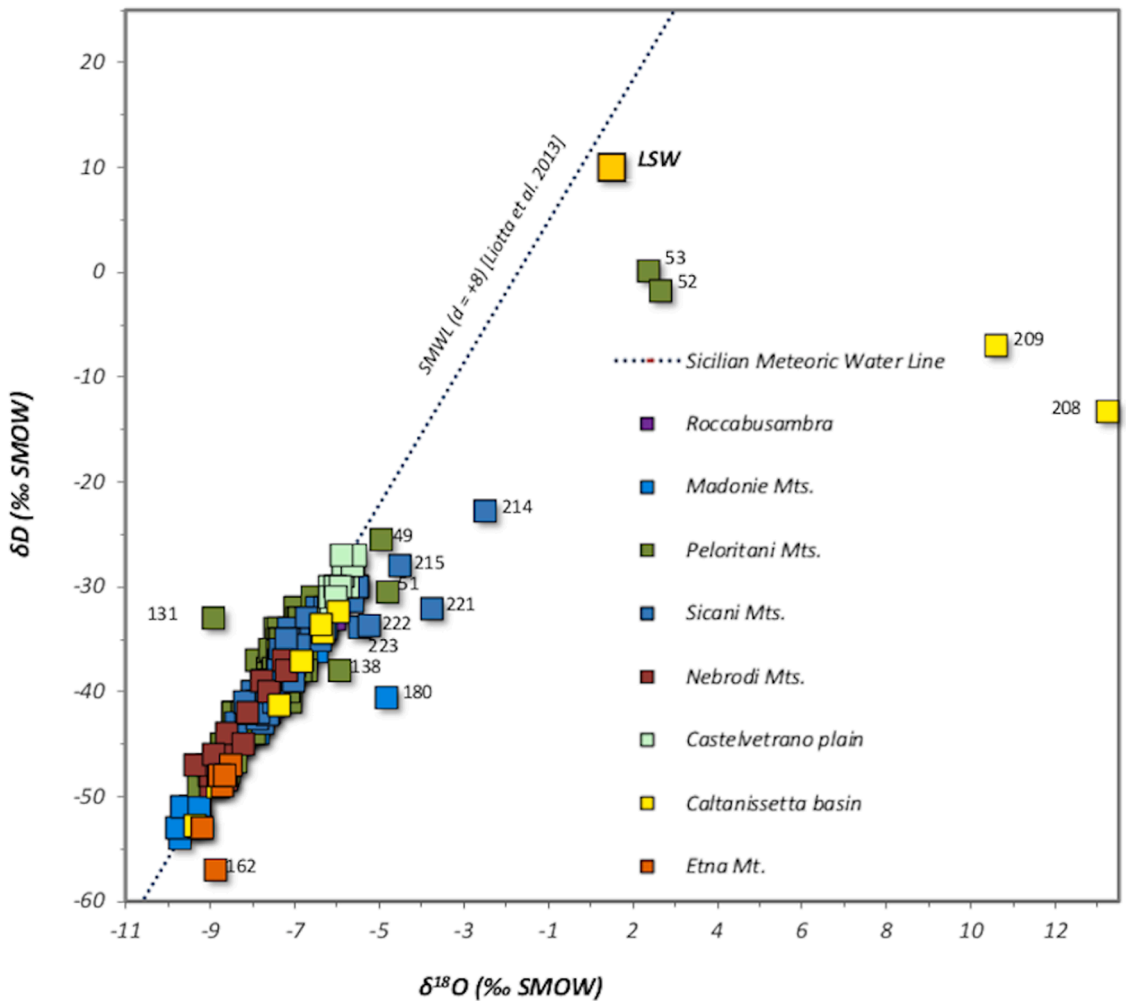

Figure 6. Diagram $\delta^{18}O$ vs. $\delta^{2}H$ of discharged waters in the study area. SMWL represents the Sicilian Meteoric Water Line (Liotta et al., 2013). LSW represents the isotopic composition of the Local Sea Water (Data references in Table 1 in supplementary material).

increase in N_2 was recorded.

Dissolved CH_4 ranged from 1×10^{-4} to 15% by vol., the highest concentrations being found in #52, #18, #48 (Peloritani Mts.), #221 and #180 (Sicani and Madonie Mts.). Argon, He, and Ne concentrations were up to 2.05%, 8×10^{-2} % and 7×10^{-2} % by vol., respectively. H_2 and CO were above the instrumental detection limit in a very limited number of samples ranging from 9×10^{-4} to 3×10^{-3} and from 1×10^{-5} to 3×10^{-5} % by vol., respectively. Gas discharges from mud volcanoes were dominated by CH_4 (from 86 to 97.5% by vol.), with minor concentrations of CO_2, N_2, O_2 and He (up to 4.0, 6.8, 2.1, and 0.04 % by vol., respectively). The $\delta^{13}C$-CO_2 values showed a wide range: from -26.52 (Roccabusambra) to -0.38 (Peloritani Mts.) ‰ *vs. PDB*. The helium isotopic composition determined in selected samples, showed significant variations with values ranging from 0.62 (#55) to 1.90 (#37) in the Peloritani Mts., from 0.41 (#221) to 1.40 (#220) in the Sicani Mts., from 0.44 (#209) to 1.31 (#208) in the Caltanissetta basin. Finally, R/Ra values of 0.70 and 2.68 R/Ra were measured in the Madonie Mts. and the Sciacca Basin, respectively.

5. Discussion

5.1. Origin of waters

Ca(Mg)-HCO_3 waters – They diffusely emerge along the whole studied area and basically consist of cold to hypothermal (<22°C) waters with TDS values up to 1,388 mg/L (except for #50 in Peloritani Mts: 2,303 mg/L), suggesting a relatively shallow water circuits as highlighted by their distribution along the Sicilian Meteoric Water Line (SMWL; Liotta et al., 2013) and consequently, markedly meteoric-originated (Fig. 6). Most waters show a stoichiometric HCO_3/(Ca+Mg) ratio and are under-saturated in calcite and aragonite (Table 3 in supplementary material), confirming a control by carbonate dissolution. The thermal waters #212 and #213 (Sciacca Basin) are over-saturated in calcite, aragonite and dolomite and under-saturated in gypsum and anhydrite, indicating processes of precipitation of carbonate minerals and dissolution of Miocene evaporites.

Na-HCO_3 waters – They have a clear meteoric origin (Fig. 6) and are widely characterizing the Peloritani Mts. waters and only two samples from the Nebrodi Mts. (#163) and Etna Mt. (#161) and have a clear. Prolonged water-rock interaction generally favors the dissolution of silicate minerals, inducing the progressive increase of Na to the waters (e.g. Grassa et al., 2006). Moreover, clay sediment-water interactions, as those recognized in the Peloritani Mts., Nebroidi Mts. and Etna Mt., a direct Ca-Na ion exchange can be induced. Na-HCO_3 waters have higher temperatures (up to 30.2°C, #32) and higher TDS (up to 6,000 mg/L) when compared with the Ca(Mg)-HCO_3 waters, supporting longer water-rock interaction processes.

Na-Cl waters – Most Na-Cl waters are hypothermal (18<T<21°C) to thermal (T> 21°C) (Table 1 in supplementary material).

Almost all thermal waters (#214, #215, #217, #219, Sciacca Basin; #180, Madonie Mts.; #49, #53, Peloritani Mts.) appear to be at equilibrium or under-saturated in aragonite, calcite and dolomite; in

addition, waters #49, #51 and #53, emerging in the Ionian sector of the Peloritani Mts. and hosted in the metamorphic aquifer, and #214, #215 and #217, discharging from the Sciacca area, are slightly gypsum and anhydrite under-saturated, underlining a possible interaction with these minerals. The Miocene evaporitic succession, consisting of selenitic gypsum and clastic-evaporitic deposits from the Mesozoic carbonatic succession hosting these thermal fluids (Fancelli et al., 1994), is indeed cropping out in the western part of the study area. Gypsum-bearing evaporitic dolomites and yellow limestones are found In the eastern sector (e.g. Alì Terme) within the Mesozoic sedimentary cover of the Mandanici metamorphic rocks (Messina et al., 2013). A few low salinity Na-Cl cold waters, i.e. #126, #155 (Peloritani Mts.) and, possibly #5 and #6, are likely related to the contribution by marine aerosols. Along the Tyrrhenian and Ionian coast of the Peloritani Mts., #18 and #52 are likely affected by interaction with seawater, as suggested their high salinity (7,720 and 40,904 mg/L, respectively, Table 1 in supplementary material) and Cl/Na>1.

The Na-Cl waters from mud volcanoes (#208, #209, #210 and #211) have a neutral to alkaline pH and high TDS (between 14,940 and 28,758 mg/L) values. According to Heller (2011), fluids discharged from mud volcanoes are probably fossil waters of marine origin. The marine geochemical properties tend to be strongly modified by both diagenetic processes and prolonged water-rock interaction processes, as shown by the relationships between solutes which are significantly different with respect to those of seawater. Moreover, enrichments in the heavier water isotopes with respect to both meteoric- and seawater-originated waters are highlighted, similarly to what identified by other studies (e.g. Dia et al., 1999; You et al., 2004, Madonia et al., 2011). It is remarkable the low content of SO_4, likely caused by bacteria reduction processes associated with the degradation of organic matter and/or anaerobic oxidation of methane (e.g. Murray et al., 1978; Capozzi et al., 2002). The reactions that facilitate a reduction of the sulfate content in solution, at which an increase of the bicarbonate content (e.g. #210) is associated (e. g. Madonia et al., 2011), are:

$$2CH_2O + SO_4^{2-} \leftrightarrow H_2S + 2HCO_3^- + H_2O$$

and

$$CH_4 + SO_4^{2-} \leftrightarrow HS^- + HCO_3^- + H_2O.$$

High SO_4 contents were only found in #208 Na-Cl(SO_4). Thermodynamic computations of these waters showed that aragonite, calcite and dolomite oversaturation increases, as follows: #209<#211<#210<#208. Therefore, the carbonate precipitation would explain the decrease of Ca and Mg in these waters at which a direct ion exchange (Na_{sol} – Ca_{clay}) cannot be excluded.

According to Trabelsi et al. (2012), the marine contribution in sampled waters can be quantified by applying the following chloride mass balance equation:

$$\%_{sea} = \left[Cl_{sample} - - Cl_{fresh}\right] / \left[Cl_{sea} - - Cl_{fresh}\right] \times 100$$

where Cl_{sample} is the concentration of Cl^- in the sample; Cl_{fresh} is the concentration of Cl^- in the less saline sample identified in the study area (0.18 meq/L); Cl_{sea} is the concentration of Cl^- in the local seawater (610 meq/L). Accordingly, the percentage of seawater ($\%_{sea}$) in the water samples close to the coastline is: ~22% (#215), ~17% (#49), ~96% (#53), ~95% (#52), ~59% (#214), ~34% (#217), ~32% (#51) and ~11% (#18). The most sea water polluted samples (#52 and #53), characterizing the Ionian sector of the Peloritani Mts. area, are enriched in both $\delta^{18}O$ and δ^2H, likely also due to additional processes such as water-rock interaction.

The thermal samples #214, #215, #221, #222, #223, #180 and #51 are enriched in ^{18}O, while the enrichment in ^2H is negligible. The $\delta^{18}O$-shift is generally attributed to isotopic exchange processes between the circulating fluids and the host rock at high temperature conditions (generally >150°C, e.g. Truesdell and Hulston, 1980). The thermal samples close to the coast (#51: Alì Terme and #214, #215: Sciacca), where a mixing with seawater was identified (Capaccioni et al., 2011), show a mixing process between a meteoric and a seawater component, the latter being isotopically modified by isotopic exchange with the host rock at temperatures exceeding 150°C (Truesdell and Hulston, 1980).

Na-SO_4(HCO_3) – Samples #26 and #37 discharging in the Tyrrhenian sector of the Peloritani Mts. showed relatively high pH and reducing conditions (-223 and -12 mV) and high Na/Cl ratios, whereas sample #172 (Nebrodi Mts.) had pH of 6.5, TDS of 112 mg/L and a positive Eh (284 mW). The SO_4 and HCO_3 contents are possibly caused by dissolution of CO_2 and H_2S produced by metamorphic rocks. The upstream gas phase makes these waters more aggressive towards the minerals, whose alteration favors the release of Na ions, according to the reaction:

$$2NaAlSi_3O_8 + 2CO_2 + 3H_2O \rightarrow Al_2Si_2O_5(OH)_4 + 2Na+ + 4SiO_2 + 2HCO_3^-.$$

The Na contents are likely also related to cationic exchange processes with clays.

Ca-Cl waters – The four waters belonging to this group (#54 and #122: Peloritani Mts., #252: Sicani Mts. and #289: Castelvetrano basin) are located close to the coast and likely mix with seawater that favors reverse cation exchange processes with clays (e.g. Zaidi et al., 2015 and references therein).

Ca(Mg)-SO_4 waters – The Ca(Mg)-SO_4 waters (#82 and #148 in the Peloritani Mts; #204, #206, #207, #201 and #203 in the Caltanissetta basin) are likely related to dissolution of sulfate minerals, being gypsum and anhydrite over-saturated (only the #201, #82 and #148 are slightly under-saturated in anhydrite). Samples #203, #207 and #204 have an SO_4-excess with respect to the stoichiometric ratio with calcium. According to Di Maggio et al. (2009), the interaction with Mg-rich salts pertaining to the Sicilian evaporitic complex can be invoked although an additional source of Mg and SO_4 could be related to dedolomitization processes, i.e. incongruent dissolution of dolomite and precipitation of calcite driven by the irreversible dissolution of gypsum. Dedolomitization proceeds until gypsum achieves saturation, resulting in an increase of Mg and SO_4 ions. The aragonite, calcite and dolomite saturation indices of #220 (Sicani Mts.) indicates that this thermal water is in equilibrium with the carbonate species, which constitute the reservoir rock (the carbonate and dolomitic Mesozoic sequence), outcropping in correspondence of the Montevago area (Montanari et al., 2014; Trumpy et al., 2015).

5.2. Geothermometry

Equilibrium reservoir temperatures of the thermal waters with T > 21°C and those from mud volcanoes were evaluated according to the Na-K-Mg system (Giggenbach, 1988). The K-Mg geothermometer quickly responds to temperature changes, whereas the Na-K geothermometer has a slower kinetics and better records temperatures attained at a greater depth. Most sampled waters plot in the field of immature water, whereas some samples from the mud volcanoes fall in the field of partially equilibrated waters (#211, #209 and #208) and one in that of full equilibrium (#210), suggesting equilibrium temperatures ranging from 80 to 120°C. Such temperatures are consistent with previous estimations of the fluid source (depth >3,000 m; Tassi et al., 2012a).

Some thermal waters tend to approach the partially equilibrated field at equilibrium temperatures between 120 to 220°C, the highest ones being computed for the western (#214, #217 and #215) and eastern sectors (#51, #53 and #49) (Figs. 3 and 7). Significantly lower temperatures (from 45°C: #221 to 138°C: #32) were obtained according to quartz solubility, likely due to dilution processes, typically affecting the silica geothermometer (Fournier, 1977). It is worth noting that when a fluid rises to the surface, it is subject to physical and chemical processes that can change its final composition. For this reason, it is necessary to use geothermometers cautiously for estimate temperature

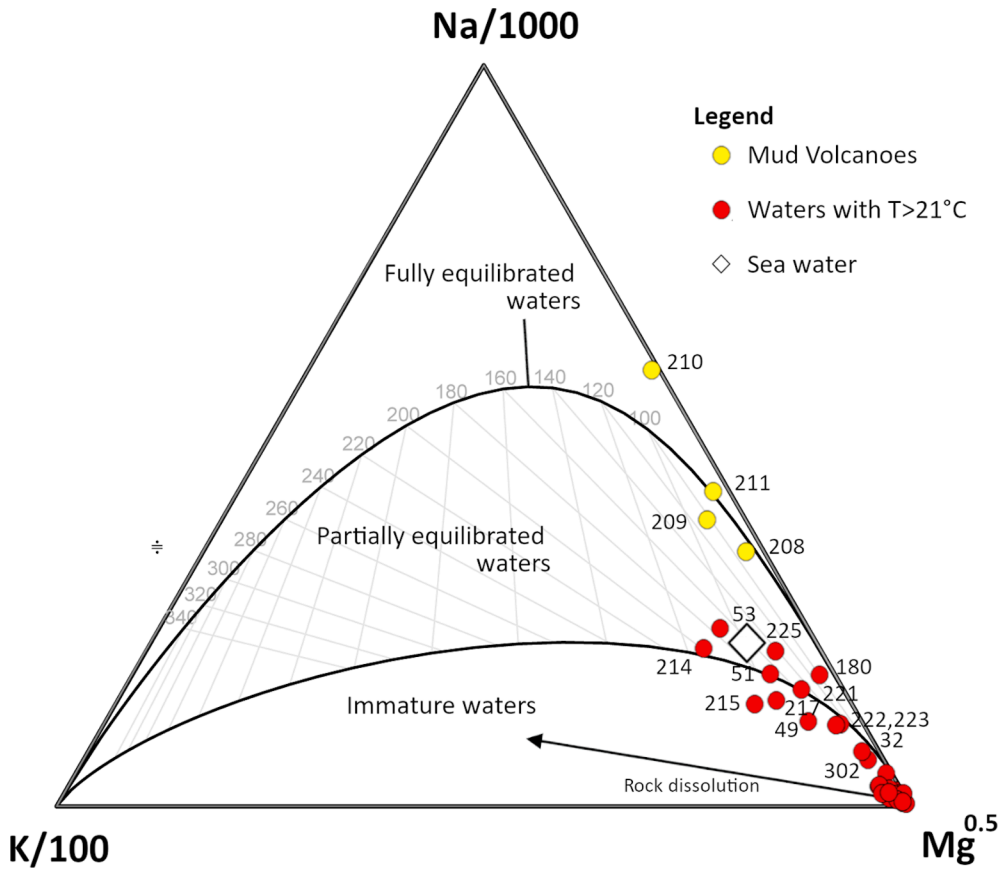

Figure 7. Na-K-Mg diagram (Giggenbach, 1988)

of hydrothermal systems (Minissale et al., 2019).

5.3. Origin of gases

Dissolved gases in thermal waters are dominantly CO_2-rich, whereas those in cold waters mostly consist of N_2 and Ar with low CO_2 content. However, some cold samples (#18, #52 and #54), discharging in areas affected by intense diffuse soil degassing along the Ionian and Tyrrhenian coastline of the Peloritani Mts. (Camarda, 2004; Giammanco et al., 2008 and Italiano et al., 2006), are characterized by high concentrations of dissolved CO_2 (≥74 % in vol.). Waters with the highest CO_2 contents have a Na-Cl composition and logpCO_2 values > -0.78 (up to 0.05) although two samples, #50 and #32, whose composition was Ca-HCO_3 and Na-HCO_3, respectively, show relatively high logpCO_2 values (-0.16 and -0.15, respectively). Cold and some thermal waters are enriched in N_2 of atmospheric origin, as marked by their N_2/Ar ratios that range from that of the air (N_2/Ar = 83) to that of air-saturated water (ASW: N_2/Ar = 38) with computed logpCO_2 values between -4.39 and -1.21.

To trace the origin of gases, the isotopic signature of CO_2 (as $\delta^{13}CCO_2$ *vs.* PDB) and He (as R/Ra only determined in selected samples) is pivotal. The main sources of CO_2 can be defined, as follows: i) thermo-metamorphic processes affecting carbonates rocks and/or the crystalline basement (-2 ≥$\delta^{13}CCO_2$ ≥2‰, Craig, 1963), ii) oxidation of organic matter (-28 ≥$\delta^{13}CCO_2$≥-13 ‰ *vs.* PDB, Cerling et al., 1991) and iii) mantle degassing (and -8 ≥$\delta^{13}CCO_2$≥ -3‰, Poreda et al., 1992, Chiodini et al., 1995b; 1999; 2000; Minissale et al., 1997b; Minissale, 2004; Frondini et al., 2008), being these components characterized by specific carbon isotopic signatures. The large carbon isotopic range (from -26.52 to -0.38 ‰) is apparently suggesting the presence of CO_2 attributable to all three possible sources of CO_2 (Fig. 8a).

CO_2-rich gases (between 52 and 99 % by vol.; red circles in Fig. 8a) are likely of deep origin whereas a thermometamorphic origin of CO_2 can be invoked for samples #53, #32 and #51 (Peloritani Mts.). In particular, the Peloritani Mts. area also includes samples #18, #19, and #52, #49 (Table 2 in supplementary material), whose isotopic carbon values are possibly indicating a mantle origin, -4.46, -4.31, -2.81 and -2.65‰, respectively). Similarly, the dissolved gases from the western sector (Sicani Mts. and Sciacca Basin) and the Madonie Mts. seem to have acquired a mantle-derived CO_2. Strongly negative $\delta^{13}C$-CO_2 values can be referred to a biogenic source in #302 (Roccabusambra), #57 (Peloritani Mts.), #183 (Madonie Mts.) and #201 (Caltanissetta basin) samples despite their relatively high content of CO_2. Carbon isotopic compositions of dissolved gases characterized by intermediate concentrations of dissolved CO_2 (orange circles in Fig. 8a) are apparently associated with a deep sourced CO_2 (#221: Sicani Mts. and #215: Sciacca Basin) and a biogenic signature (#59, #39, #46, #47, #60, #61, #40, #48, #7, #43 and #227: Peloritani Mts.), respectively. Samples along the Tyrrhenian sector of the Peloritani Mts. (#33 and #35) showed $\delta^{13}C$-CO_2 values of -11.23 and -12.86‰ vs. PDB, respectively, may be affected by mantle component diluted by a superficial (biogenic) source.

Finally, samples with low CO_2 content (<20% in volume, yellow circles in Fig. 8a) the biogenic component is prevailing with the exception of samples #44 (Peloritani Mts., Tyrrhenian coast), #219 (Sicani Mts.), #210 and #209 (Caltanissetta basin). In particular, #44 is apparently associated with thermometamorphic processes, whereas #219, #210 and #209 seem to be affected by a mantle contribution. It is to note that carbon dioxide emitted by mud volcanoes (#209 and #210) is generally related to a common crustal source (e.g. Tassi et al., 2012b) and is rather peculiar to record $\delta^{13}C$-CO_2 values approaching those of a mantle source. According to Tassi et al. (2012b), the production of CO_2 in CH_4-rich gases is often due to anaerobic oxidation of heavy hydrocarbons, in many cases followed by secondary methanogenesis

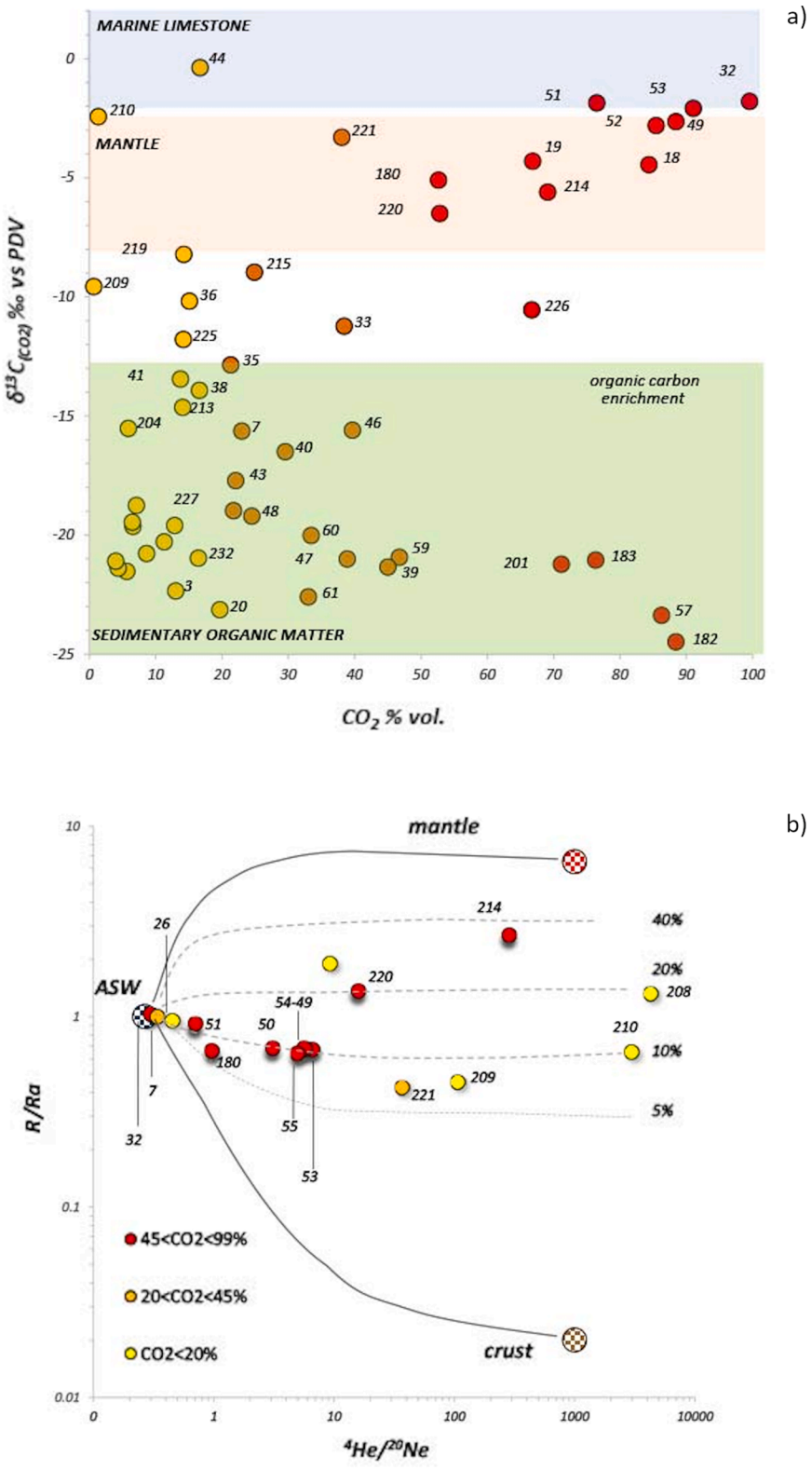

Figure 8. a) CO_2 vs. $\delta^{13}C$-CO_2 diagram. The ranges of main sources of CO_2 are shown (see text). Red circles=CO_2>52% vol; orange circles= 21>CO_2<45% vol; yellow circles = CO_2 <20% vol (Data references in Table 1 in supplementary material). b) Diagram R/Ra vs. $^4He/^{20}Ne$. The three end-member atmosphere/crust/mantle are reported as reference.

processes, which can enrich the residual CO_2 in ^{13}C (Pallasser, 2000, Etiope et al., 2009). CO_2, being much more soluble in water than CH_4, is subjected to isotopic fractionation processes linked to the interaction between upward fluids and shallow aquifers, contributing to the variation of $\delta^{13}C$-CO_2 values (e.g. Venturi et al., 2019). Therefore, the isotopic variations observed in the CH_4-rich samples from the Caltanissetta basin, are likely deriving by mixing processes at different degrees of biogenic, mantle and thermometamorphic components unless

secondary processes, during the ascent of the gas phase to the source, may significantly have modified the pristine signature (Venturi et al., 2019 and references therein).

Since no isotopic data of CH_4 are available for the other dissolved gases we cannot speculate whether the dominant component is biogenic or thermogenic. In samples #221 (Sicani Mts.) and #180 (Madonie Mts.), collected at the borders of the thick sedimentary sequence filling the Caltanissetta basin, the high concentrations of CH_4 (from 8.0 to 15% by vol.) in dissolved gases seem to be related to a thermogenic source (Tassi et al. 2012a) similar to that feeding the mud volcanoes. The latter have CH_4 originated by organic material placed at > 3,000 m depth, in a genetic environment characterized by high pressures and temperatures in the range of 100-120°C (Etiope et al., 2002; Grassa et al., 2004; Tassi et al., 2012a).

CH_4-rich samples from mud volcanoes have high helium contents, typical of long residence times at depth, thus favoring a considerable production of ^4He. On the contrary, gases from thermal springs show relatively significantly lower helium abundances, such as those that characterize the central-northern Apennines (Minissale et al., 2000). The R/Ra ratios are between 0.41 to 2.68 with $^4He/^{20}Ne$ ratios from 0.30 to 287. Considering that distinct isotopic ratios characterize i) air (R/Ra= 1), ii) crust (R/Ra ~0.02 and iii) mantle (R/Ra= ~8, Sano and Wakita, 1985), the measured R/Ra values are higher than those typically expected in the crust, suggesting significant contribution of helium from a mantle source.

By plotting the R/Ra ratios vs. $^4He/^{20}Ne$ (Fig. 8b), helium results to

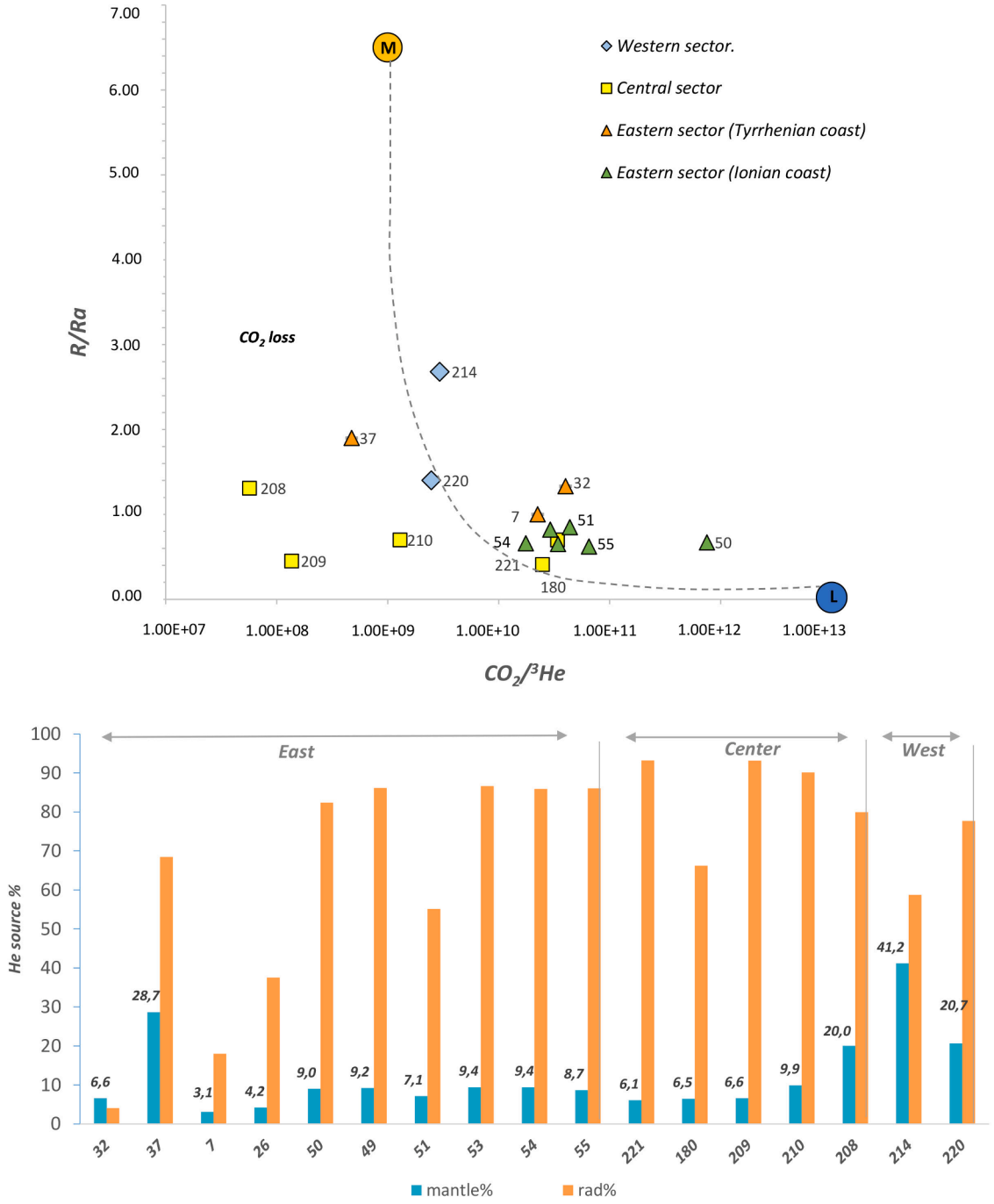

Figure 9. a) $CO_2/^3He$ vs. R/Ra plots as a function of the areal distribution of the samples. The crustal (L), and mantle (M) end-members are reported as reference; b) Geographical distribution of helium from mantle and crustal source. The percentage was calculated using the equation of Sano and Wakita (1985).

be sourced from a mixing between mantle (^{3}He), crustal (^{4}He) and atmospheric helium in different proportions. Some samples from the Tyrrhenian coast of the Peloritani Mts. area (#26, #7 and #32), the ^{4}He/^{20}Ne ratios are <0.5, approaching that of the atmosphere (0.268). On the basis of the R/Ra and ^{4}He/^{20}Ne ratios in the crust (0.02 and 1000, respectively), MORB-type mantle (8±1 and 1000) and atmosphere (1 and 0.268; Yuce et al., 2014), it is possible to estimate the contribution of the different sources, according to Sano and Wakita (1985), as follows:

$$(^3He/^4He) = (^3He/^4He)a \times A + (^3He/^4He)m \times M + (^3He/^4He)r \times R$$
$$1/(^4He/^{20}Ne) = A/(^4He/^{20}Ne)a + S/(^4He/^{20}Ne)m + R(^4He/^{20}Ne)r$$
$$A + M + R = 1$$

where a, m and r represent atmospheric, mantle and radiogenic He, respectively, whilst A, M and R refer to the fraction of the considered reservoirs. However, instead of using a MORB-type mantle as a deep end-member, we preferred to use SCLM (Sub-Continental Lithospheric Mantle, R/Ra = 6.5) since Dunai and Baur (1995), Gautheron et al. (2005), Shimizu et al. (2005), Torfstein et al. (2013) and Yuce et al., (2014) showed the European Sub-Continental Lithospheric Mantle has a lower R/Ra, being metasomatized by subduction fluids. The estimated contribution from each end-member is shown in Fig. 8b.

Most samples show a dominant contribution of radiogenic helium (in the range: 4-93%), while that SCLM is from 3 to 41%. The highest contribution of ^{3}He (mag%= 41), supported by a high ^{4}He/^{20}Ne ratio (287), is recorded for the samples collected from the Sciacca Basin. Figure 9 shows how the percentage of mantle helium measured in the fluids varies according to the areal distribution of the samples. The western sector is indeed characterized by the highest percentages of mantle helium (from 21 to 41%), as already highlighted by Caracausi et al., (2005) and Capaccioni et al. (2011). In addition, samples #220 and #214 had isotopic carbon data within the range of mantle CO_2 at which relatively high helium isotopic values are associated.

From the western sector towards the inner part of the study area, the radiogenic component tends to increase (66 - 93%), while that of mantle are abruptly decreasing. In #208, the measured helium isotopic value (1.31Ra) is much higher than that commonly determined in CH_4-rich fluids from Northern Apennines (Minissale et al., 2000).

The contribution of mantle helium for this sample is about 20% and similar to the estimated percentage in the western sector. Within the Neogene basin, the contribution of mantle helium significantly decreases (~10%). Much lower percentages of mantle helium (~6%) were computed from the dissolved gases of #180, #221 and #209. In the eastern sector (Peloritani Mts. area), significant differences for the dissolved gases discharging from the Ionian and Tyrrhenian coastal areas are observed. Samples from the Ionian sector have a rather constant R/Ra ratios (between 0.62 and 0.85Ra) with a mantle-derived fraction <10% whereas those from the Tyrrhenian side are higher: between 0.86 and 1.33Ra but with very low ^{4}He/^{20}Ne ratios, suggesting a predominant atmospheric component (58-89 %) and a mantle helium <10%, with the exception of #32, for which a contribution of mantle helium of 30% was computed (Giammanco et al., 2008). It is to mention that near Capo Calavà, Sano et al. (1989) measured 2.5 Ra in a sample a few hundred meters from #7 and about 20 km away from #32 and #37. The highest percentages of ^{3}He were determined in the western and eastern (Tyrrhenian coast) sectors, which are regarded as those zones where the two major heat flow anomalies within the study area were observed (Cataldi et al., 1995). To better highlight the two "anomalous" mantle helium areas, the R/Ra vs. the CO_2/^{3}He ratios are plotted in Fig. 9a according to the geographical distribution of the studied gases. This diagram is consistent with that of Fig. 9b, where the percentage of mantle and crustal helium is geographically plotted. The largest contribution from a mantle source is in the western sector, while the lowest one refers to the fluids discharged in the central sector of the study area.

Only samples #210 (central sector of the study area), #220 and #214 (western sector) (Fig. 9b) show R/Ra ratios that fall within the typical range of mantle fluids (Marty and Jambon, 1987; O'Nions and Oxburgh, 1988; Hooker et al., 1985). Some important information can be obtained by plotting the CO_2 and δ^{13}C-CO_2 vs. the CO_2/^{3}He ratio (Figs. 10 a and b).

For the other samples, the CO_2/^{3}He ratios (Fig. 10a) seem to confirm the predominant crustal origin of CO_2, although a contribution of a deeper, mantle-like source is observed in Fig. 10b where samples distribute along the mixing line between the Mantle and Limestone endmembers. In samples #55, #50 and #54 (no δ^{13}C-CO_2 data, Fig. 10, Table 2 in supplementary material), the CO_2/^{3}He ratio highlights a predominantly crustal origin. Samples #209, #208 (Caltanissetta basin) and #37 (Tyrrhenian coast of Peloritani Mts. area) have the lowest CO_2/^{3}He ratios and fall below the Mantle endmember (Figs. 10a, b), being a direct consequence of CO_2 loss and/or He acquisition (Marty & Jambon, 1987). Due to the great difference in solubility between these two gas species, the interaction between deep gas phase and shallow aquifers could lead to a preferential dissolution of the most soluble species (CO_2). This process involves a progressive decrease in CO_2 content while the less soluble species (He) enriches. This process, already suggested by Giammanco et al. (2008), may allow to explain the low concentration of CO_2 and the high concentration of He in solution in the sample #37. The loss of CO_2 and the enrichment in ^{4}He is also noticeable in the CH_4 manifestations characterizing the Caltanissetta basin.

6. Fluid geochemistry vs. tectonics

The complex geodynamic setting characterizing the Central Mediterranean area derives by the interaction between the European and African domains. This sector of the Apenninic-Maghrebian chain is located between two important extensional areas: the Sicily Channel to the south and the Tyrrhenian sea back-arc basin to the north. The compressive regime predominatly characterizes the central and southern parts of the study area. Conversely, the northern part (e.g. Peloritani sector) is currently affected by extensive tectonics, as highlighted by Carminati & Doglioni (2012). Strike-slip tectonics is recognized in different sectors of the study area (Barreca et al., 2016; Carafa & Barba 2013).

Heat flow values >200 mW/m^2 were measured by Cataldi et al. (1995) in the Tyrrhenian basin and the Sicily Channel. Lower values were computed in the mainland with relatively anomalous values (around 65-70 and 70 mW/m^2) in the Sciacca Basin and between the Madonie and Nebrodi Mts. Here, areas with higher heat flow are corresponding to those characterized by higher R/Ra ratio, except for the Peloritani sector. We stress that the occurrence of ^{3}He can generally be related to the presence of deep magmas intruded into the crust and/or deep faults with extensional component (e.g. Caracausi et al., 2013, D'Alessandro et al., 2014, Yuce et al., 2014). On the contrary, the Sciacca Basin and the surrounding areas toward Montevago and the Caltanissetta Basin are characterized by a dominating compressive tectonics and high R/Ra values (>0.42 up to 2.68 Ra). To justify the recorded high R/Ra values regional tectonic structures, able to act as a preferential way for the ascent of heat and deep-seated (magma) fluids to the surface, are to be assumed.

The goal of this work is to depict the conceptual model of the study area integrating the available dataset. From a geodynamic and geochemical point of view, three major domains can be distinguished: western, central and eastern and for each of them a schematic conceptual model of fluid circulation to explain the main geochemical and isotopic features of the studied water and gas phases was proposed.

According to Montanari et al. (2017), the presence of a regional geothermal reservoir within the Mesozoic carbonate units was identified. The reservoir shows a typical arrangement in structural highs and lows resulting by the regional tectonic evolution. The geometry of the

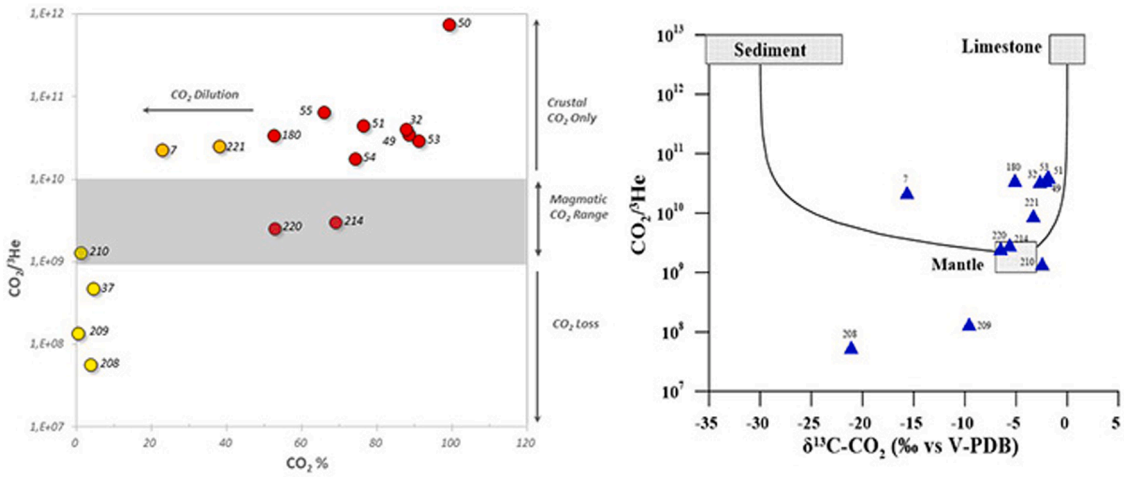

Figure 10. a) $CO_2/^3He$ vs. CO_2 % in vol. for selected gas data. The shade region highlights the magmatic CO_2 range; b) $\delta^{13}C$-CO_2 vs $CO_2/^3He$. The black plot. The black lines represent the mixing lines among sediment, mantle (MORB) and limestone endmembers by Sano and Marty (1995).

top of the reservoir is from Montanari et al. (2014) whereas the reservoir thickness for each area was defined by aeromagnetic surveys at a national scale (Cassano et al., 1986). The structural arrangement of the magnetic basement allowed to establish the deepest level below which the presence of sedimentary rocks can be excluded.

In the western sector of the study area (Fig. 11a), the sedimentary succession (Mesozoic limestone and dolomite) is close to the surface and in several areas, it is outcropping, likely representing the recharge areas of the deep thermal system. In this sector, the Mesozoic reservoir is 7-8 km thick and is overlain by a thick Neogene-Quaternary terrigenous, clastic and evaporitic sequence. The latter acts as an impermeable cover for the geothermal system reservoir, due to its low permeability. It is to mention that multi-layer aquifers are occasionally present and separated by impermeable horizons. These shallow aquifers occur in both the conglomeratic and/or sandy layers belonging to the Messinian evaporites and the Plio-Pleistocene sandy/conglomeratic levels (e.g. Favara et al., 1998). The western sector hosts two important hydrothermal systems: Montevago and Sciacca (e.g. Alaimo et al. 1978; Grassa et al., 2006; Capaccioni et al., 2011), which show compositional and isotopic differences in the water and gas phase. The water chemistry of Montevago system is due to mixing processes of three components: i) carbonate (resulting from the dissolution of calcite and dolomite that constitute the geothermal reservoir), ii) sulfate (due to the dissolution of gypsum that characterizes the base of the thermal reservoir) and iii) chloride (related to the interaction between seawater and shallower aquifers during the ascent to the surface). The isotopic composition of the Montevago thermal waters is comparable with a local meteoric recharge. The ascent of the thermal fluids seems to be related to a NW-SE trending fault system that dominates the Belice Valley. This observation is supported by Favara et al. (2001) who documented a direct connection between hydrothermal circulation and tectonic structures, highlighting significant variations in water chemistry over time in correspondence with seismic events, particularly during and after the catastrophic seismic event of 1968 (Monaco et al., 1996 and references therein).

Tectonic discontinuities represent the main pathways of the gas phase that may be originated at (mantle) depth. The isotopic composition of CO_2 and He (the highest R/Ra ratios among all the study samples with values of 2.68 and 1.4 for Sciacca and Montevago, respectively) indicates a contribution by deep seated magmatic intrusions and diluted by a crustal component. In the coastal area in front of the Sicily channel, three main thermal water discharges (#214, #215 and #217, the latter disappeared after the 1968 seismic event) are dominated by a Na-Cl composition, which are associated with seawater intrusion at various degrees. Other emergences in the Sciacca area (#212, #213 and #216) showed lower salinity and a Ca-HCO_3 facies to be ascribed to shallower circuits. The water isotopes are apparently confirming the presence of a high enthalpy geothermal fluid inside the deep portions of the Mesozoic carbonates, as displayed by the $\delta^{18}O$-shift, generally attributed to the isotopic exchange between circulating fluid at high temperature conditions. This is also supported by the geothermometric calculations that provided temperatures between 200 and 220°C. In agreement with previous studies (Caracausi et al., 2005; Capaccioni et al. 2011), deep fault systems are likely playing a pivotal role in transferring the mantle signature and the heat at the surface. The presence of magmatic intrusions in this area is also supported by the two eruptions that occurred in 1831 (Gemmellaro, 1831), which formed the Ferdinandea Island or Bank of Graham, and 1891 (Washington, 1909) off NW Pantelleria Island, in the Sicily Channel.

A conceptual model of fluid circulation in the westernmost part of the study area is reported in Figure 11a.

Moving to the Caltanissetta Basin, in the central sector of the study area, the top of the carbonate succession is much deeper (up to 7 km depth; Fig. 11b). This area is characterized by the presence of mud volcanoes, which are the surface expression of the accretion prism that developed in the front of the Apennine–Maghrebide fold-and-thrust belt (Bonini, 2009). They originated inside the Neogene-Quaternary terrigenous sediments that fill the Caltanissetta Basin at a high deposition rate and overlap the Mesozoic carbonate sequence. The increased interstitial pressure inside the terrigenous deposits reduced the internal volumes with consequent expulsion of water, gas and mud from the sediments, thus leading to the formation of typical sedimentary volcanoes whose activity may produce methane- and mud-rich eruptions. Paroxysmal activities were recently recorded in 2008 and 2014 (Cangemi and Madonia, 2014; Madonia et al., 2011). The liquid phase released from the mud volcanoes is a fossil (Na-Cl) chemically and isotopically modified seawater water while the gas phase is CH_4-dominated (up to 97.5 % by vol.) and thermogenically-originated at >3,000 m depth with temperatures between 100 and 120°C (Grassa et al., 2004; Tassi et al., 2012a). In this sector, although dominated by compressive tectonics, a contribution deriving from mantellic fluids was recognized since the R/Ra values were of 0.4 and 0.7. Consequently, the presence of primordial helium can be related to regional crustal fractures extending to great depths and acting as a preferential pathway of mantle and crustal fluids. At the borders of the Caltanissetta Basin, where the carbonate reservoir is outcropping in correspondence with the structural highs, the Na-Cl thermal springs of Sclafani Bagni spring (#180), emerging in the Madonie Mts. sector, occur. The helium isotopes are similar to those

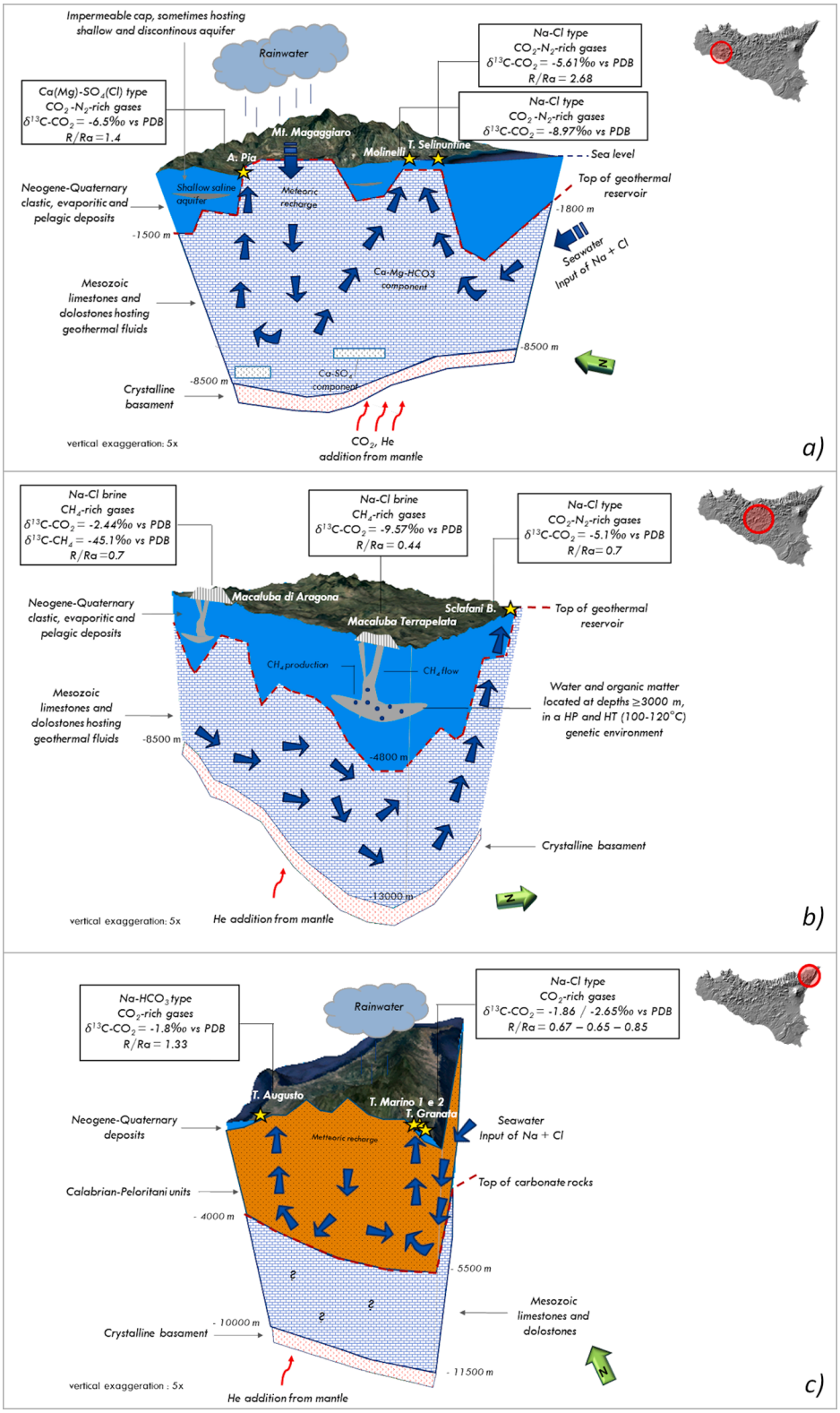

Figure 11. Conceptual geochemical model of deep water circulation in the western sector (a), central sector (b) and eastern (c) of the study area. The location of the main thermal waters is reported. The reconstruction of the top geothermal reservoir is based on the study by Montanari et al. (2014). Trend and depth of the crystalline basement are derived from Cassano et al. (1986). The rectangles at the base of the Mesozoic carbonate sequence are chalky lenses inside the reservoir.

recorded for the mud volcanoes while, according to liquid geothermometry, equilibrium temperatures of about 120°C were computed.

Within the "European element", the Calabro-Peloritan Arc, the hydrothermal circulation is governed by two important fault systems that characterize the Tyrrhenian and the Ionian coasts (Fig. 11c). Geodynamic studies (e.g. Roure et al., 1990; Montanari et al., 2014) suggested a continuity of the Apennines-Maghrebian carbonatic units below the Calabro-Peloritan Arc, which overlapped each other in the

Langhian-Tortonian. According to Montanari et al. (2014), the carbonate platform is relatively deep (up to 6 km depth) and geochemical evidences would seem to support the hypothesis of a hydrothermal circulation that affects the metamorphic rocks constituting the Peloritan area. As already mentioned, there are two main hydrothermal systems in this sector of the chain: one in the Tyrrhenian coastal sector, e.g. the Terme Vigliatore thermal system, and the other in the Ionian sector, e.g. the Alì Terme thermal system. They are related to two important fault systems: a) the NW-SE-oriented Aeolian-Tindari-Letojanni fault system and b) the NE-SW-oriented Messina System.

The water discharges from the Tyrrhenian and Ionian sectors showed distinct geochemical features, the former being mostly characterized by Na-HCO_3 waters, indicating the presence of CO_2-rich gas phase that favors the chemical alteration of the silicate minerals belonging to the metamorphic formations. The latter are Na-Cl due to mixing processes with seawater. Both thermal systems are fed by meteoric waters. The waters of the Ionian sector lie to the right side of the LMWL likely due to evaporation. In both areas, a slight contribution (up to 28%) by a mantle source was recognized in the Tyrrhenian sector whilst it decreased down to < 10% in the Ionian sector. Liquid geothermometers allowed to estimate equilibrium temperatures up to 180°C.

7. Conclusions

The NE-SW-oriented geochemical transect investigated in the present study highlighted the presence of several thermal fluid manifestations such as thermal waters, mud volcanoes and bubbling pools, whose related waters showed a large variability in terms of chemical and isotopic composition. This large variability is likely reflecting the complex geological-structural setting of the Sicilian territory and associated with processes of i) water-rock-gas interaction at low to high (>150°C) temperatures; ii) direct and reverse ion exchanges and iii) mixing between deep and shallow aquifers and seawater. The dissolved and free gas geochemistry showed that the western and central-northern sector of the study area was CO_2-N_2 dominated whereas the central part, where the mud volcanoes are discharging, was characterized by typical CH_4-rich gas emissions. While the geothermal reservoir in the central and western sectors of Sicily is located inside the Mesozoic carbonates, overlain by a thick impermeable sedimentary sequence minimizing the deepest geochemical signal at the surface, in the eastern sector, the Peloritan crystalline basement is likely hosting a CO_2-rich gas phase thermal reservoir. All the thermal emergences discharge in correspondence of important tectonic discontinuities.

On the basis of carbon and helium isotopes, significant contributions of mantle-derived gases were recognized in the western sector of Sicily, as already highlighted by numerous scientific studies (e.g. Grassa, 2004; Caracausi et al., 2005; Grassa et al., 2006), and in the central-western and central sector of the study area, including the gas discharges associated with the release of methane. This geochemical vs. structural observation is likely responsible of the relatively high reservoir temperature (up to 220°C) estimated by liquid geothermometry. Even though towards SW the thermal systems from Sicily are mostly characterized by compressive tectonics, the occurrence of significant mantle He is likely caused by fault systems that favor the uprising of deep originated gases.

New hints on the geothermal reservoirs in the Sicilian mainland are provided. A geochemical characterization of different type of deep fluids is proposed and related to the different geological settings. In addition to the well-known geometries of the regional carbonate reservoir in the central and western sectors and their shallow temperatures (usually <120°C), we suggest the presence of deeper high temperature conditions. The hydrothermal circulation in metamorphic units in the eastern sector of the study area was constrained in detail. The regional economy would importantly benefit by the use of geothermal energy for both the production of electricity or medium-to-low enthalpy applications. Nevertheless, the present study is intended to serve as a basis for future research activities in the area although further scientific investigations are required to better assess the structure of the geothermal reservoirs.

Author statement

Assunta Donato: Conceptualization, Formal analysis, Investigation, Writing Original Draft, Review and Editing, Visualization.

Franco Tassi: Conceptualization, Validation, Resources, Writing Original Draft, Review and Editing, Supervision.

Giovannella Pecoraino: Conceptualization, Investigation, Resources, Writing Original Draft, Review and Editing.

Adele Manzella: Conceptualization, Supervision, Project administration, Funding.

Orlando Vaselli: Conceptualization, Validation, Resources, Writing Original Draft, Review and Editing, Supervision.

Esterina Gagliano Candela: Investigation, Project administration.

Alessandro Santilano: Writing Original Draft, Review and Editing, Visualization.

Leonardo La Pica: Investigation.

Claudio Scaletta: Investigation.

Francesco Capecchiacci: Investigation, Formal analysis.

Declaration of Competing Interest

The authors declare that they have no known competing financial interests or personal relationships that could have appeared to influence the work reported in this paper.

Acknowledgements

The authors wish to thank the Head of Isotope Chemistry Laboratory of CNR-IGG (Eng. Mario Mussi, CNR-IGG) and Enrico Calvi and the Head of Laboratory of INGV-Section of Palermo (Dr. Andrea L. Rizzo) and the respective teams are warmly thanked for their support during the analytical work.

Yuri Taran and an anonymous reviewer are gratefully acknowledged for their useful comments and suggestions that strongly improved an early version of the manuscript.

This work benefited from the financial support of the VIGOR ("Valutazione del potenzIale Geotermico delle regiOni della conveRgenza", i.e. Geothermal potential assessment of Regioni Convergenza) and Geothermal Atlas of southern Italy projects, of the Regione Siciliana, Commissario Delegato per l'Emergenza Bonifiche e la Tutela delle Acque in Sicilia which funded and commissioned INGV-Sezione di Palermo for the redaction of the Piano di Tutela delle Acque della Sicilia (2007) and the Laboratories of Fluid Geochemistry (FT) and Laboratory of Stable Isotopes (OV) of the Department of Earth Sciences of Florence.

Supplementary materials

Supplementary material associated with this article can be found, in the online version, at doi:10.1016/j.geothermics.2021.102120.

References

Accaino, F., Catalano, R., Di Marzo, L., Giustiniani, M., Tinivella, U., Nicolich, R., Sulli, A., Valenti, V., Manetti, P., 2011. A crustal seismic profile across Sicily. Tectonophysics 508, 52–61.

Aiuppa, A, Allard, P, D'Alessandro, W, Michel, A, Parello, F, Treuil, M, and Valenza, M. Mobility and fluxes of major, minor and trace metals during basalt weathering and groundwater transport at Mt. Etna volcano (Sicily). United States: N. p., 2000. Web. doi:10.1016/S0016-7037(00)00345-8.

Alaimo, R., Carapezza, M., Dongarrà, G., Hauser, S., 1978. Geochimica delle sorgenti termali siciliane. Rend. Soc. It. Min. Petrol. 34, 577–590 (In Italian with English abstract).

Amodio-Morelli, L., Bonardi, G., Colonna, V., Dietrich, D., Giunta, G., Ippolito, F., Liguori, V., Lorenzoni, V., Paglionico, A., Perrone, V., Picaretta, G., Russo, M., Scandone, P., Zanetti-Lorenzoni, E., Zuppetta, A., 1976. L'arco Calabro-Peloritano

nell'orogene appenninico-maghrebide. Mem. Soc. Geol. It. 17, 1–60 (In Italian with English abstract).
Anderson, H., Jackson, J., 1987. The deep seismicity of the Tyrrhenian Sea. Geophys. J. Royal Astron. Soc. 91, 613–637.
Barreca, G., Scarfì, L., Cannavò, F., Koulakov, I., Monaco, C., 2016. New structural and seismological evidence and interpretation of a lithospheric-scale shear zone at the southern edge of the Ionian subduction system (central-eastern Sicily, Italy). Tectonics 35, 1489–1505. https://doi.org/10.1002/2015TC004057.
Bello, M., Franchino, A., Merlini, S., 2000. Structural model of Eastern Sicily. Mem. Soc. Geol. It. 55, 61–70 (In Italian with English abstract).
Benavente, O., Tassi, F., Reicha, M., Aguilera, F., Capecchiacci, F., Gutiérrez, F., Vaselli, O., Rizzo, A., 2016. Chemical and isotopic features of cold and thermal fluids discharged in the Southern Volcanic Zone between 32.5°S and 36°S: Insights into the physical and chemical processes controlling fluid geochemistry in geothermal systems of Central Chile. Chem. Geol. 420, 97–113.
Bonini, M., 2009. Mud volcano eruptions and earthquakes in the Northern Apennines and Sicily, Italy. Tectonophysics 474, 723–735.
Brusca, L., Aiuppa, A., D'Alessandro, W., Parello, F., Allard, P., Michel, A., 2001. Geochemical mapping of magmatic gas–water–rock interactions in the aquifer of Mount Etna volcano. Journal of Volcanology and Geothermal Research 108, 199–218.
Butler, R.W.H., Grasso, M., 1993. Tectonic controls on base-level variations and depositional sequences within thrust-top and foredeep basins: examples from the Neogene thrust belt of central Sicily. Basin Res 5, 137–151.
Butler, R.W.H., Lickorish, W.H., Grasso, M., Pedley, H.M., Ramberti, L., 1995. Tectonics and sequence stratigraphy in Messinian basins, Sicily: Constraints on the initiation and termination of the Mediterranean salinity crisis. Geol. Soc. Am. Bull. 107, 425–439.
Camarda, M., 2004. Soil CO2 Flux Measurements in Volcanic and Seismic Areas: Laboratory Experiments and Field Applications. PhD Thesis. University of Palermo (Italy.
Cangemi, M., Madonia, P., 2014. Mud volcanoes in onshore Sicily: a short overview. Gottingen Contrib. Geosci. 77, 123–127.
Capaccioni, B., Vaselli, O., Tassi, F., Santo, A.P., Delgado Huertas, A., 2011. Hydrogeochemistry of the thermal waters from the Sciacca Geothermal Field (Sicily, southern Italy). J. Hydrol. 396, 292–301.
Capozzi, R., Picotti, V., 2002. Fluid migration and origin of a mud volcano in the northern Apennines (Italy): the role of deeply rooted normal faults. Terra Nova 14, 363–370.
Caracausi, A., Favara, R., Italiano, F., Nuccio, P.M., Paonita, A., Rizzo, A., 2005. Active geodynamics of the central Mediterranean Sea: Tensional tectonic evidences in western Sicily from mantle derived helium. Geophys. Res. Letters 32, L04312. https://doi.org/10.1029/2004GL021608.
Caracausi, A., Martelli, M., Nuccio, P.M., Paternoster, M., Stuart, F.M., 2013. Active degassing of mantle-derived fluid: A geochemical study along the Vulture line, southern Apennines (Italy). J. Volcanol. Geotherm. Res. 253, 65–74.
Carafa, M.M.C., Barba, S., 2013. The stress field in Europe: optimal orientations with confidence limits Geophys. J. Intl. 193, 531–548.
Carapezza, M., Cusimano, G., Liguori, V., Alaimo, R., Dongarrà, G., Hauser, S., 1977. Nota introduttiva allo studio delle sorgenti termali dell'isola di Sicilia. Boll. Soc. Geol. It. 96, 813–836. In Italian with English abstract.
Carminati, E., Doglioni, C., 2012. Alps vs. Apennines: The paradigm of a tectonically asymmetric Earth. Earth Sci. Rev. 112, 67–96.
Cassano, E., Fichera, R., Arisi Rota, F., 1986. Rilievo aeromagnetico d'Italia: alcuni risultati interpretative. In: Proceed. 5th Congress of the Gruppo Nazionale di Geofisica della Terra Solida, 17-19 November, 1986. Rome, Italy.
Catalano, R., 2004. Geology of Sicily: An introduction. BOCCONEA 17, 33–46.
Catalano, R., D'Argenio, B., 1978. An essay of palinspastic restoration across western Sicily. Geol. Romana 17, 145–159.
Catalano R., D'Argenio B., 1982. Schema Geologico della Sicilia. In: Catalano R. & D'Argenio B.(eds) Guida alla geologia della Sicilia occidentale. Mem. Soc. Geol. It. (Suppl. A), 9–41. (In Italian with English abstract).
Catalano, R., Di Stefano, P., Sulli, A., Vitale, F.P., 1996. Paleogeography and structure of the central Mediterranean: Sicily and its offshore area. Tectonophysics 260, 291–323.
Catalano, R., Franchino, A., Merlini, S., Sulli, A., 2000a. A crustal section from North Algeria to the Ionian ocean (Central Mediterranean). Mem. Soc. Geol. It. 55, 71–85.
Catalano, R., Valenti, V., Albanese, C., Accaino, F., Sulli, A., Tinivella, U., Gasparo Morticelli, M., Zanolla, C., Giustiniani, M., 2013. Sicily 'fold-trhust belt and slab roll-back: the SI.RI.PRO. seismic crustal transect. J. Geol. Soc. London. https://doi.org/10.1144/jgs2012-099.
Cataldi, R., Mongelli, F., Squarci, P., Taffi, L., Zito, G., Calore, C., 1995. Geothermal ranking of Italian territory. Geothermics 24, 115–129.
Cerling, T.E., Solomon, D.K., Quadev, Bowman J.R., 1991. On the isotopic composition of carbon in soil carbon dioxide. Geochim. Cosmochim. Acta 55, 3403–3405.
Cheng, W., Kuo, T., Su, C., Chen, C., Fan, K., Liang, H., Han, Y., 2010. Evaluation of natural recharge of Chingshui geothermal reservoir using tritium as a tracer. Rad. Measur. 45, 110–117.
Chiodini, G., Allard, P., Caliro, S., Parello, F., 2000. ^{18}O Exchange between steam and carbon dioxide in volcanic and hydrothermal gases: Implications for the source of water. Geochim. Cosmochim. Acta 64, 2479–2488.
Chiodini, G., Frondini, F., Kerrick, D.M., Rogie, J., Parello, F., Peruzzi, L., Zanzari, A.R., 1999. Quantification of deep CO_2 fluxes from Central Italy. Examples of carbon balance for regional aquifers and of soil diffuse degassing. Chem. Geol. 159, 205–222.
Chiodini, G., Frondini, F., Ponziani, F., 1995b. Deep structures and carbon dioxide degassing in central Italy. Geothermics 24, 81–94.
Craig H., 1963. The Isotopic Geochemistry of Water and Carbon in Geothermal Areas. In: Tongiorgi E. (Ed.), Nuclear Geology on Geothermal Areas. CNR (Italian Council for Research), Spoleto, Italy, pp. 17–54.
D'Alessandro, W., Brusca, L., Kyriakopoulos, K., Bellomo, S., Calabrese, S., 2014. A geochemical traverse along the "Sperchios Basin — Evoikos Gulf" Graben (Central Greece): origin and evolution of the emitted fluids. Mar. Petrol. Geol. https://doi.org/10.1016/j.marpetgeo.2013.12.011.
De Siena, L., Chiodini, G., Vilardo, G., Del Pezzo, E., Castellano, M., Colombelli, S., Tisato, N., Ventura, G., 2017. Source and dynamics of a volcanic caldera unrest: Campi Flegrei, 1983–84. Scientific Reports 7, 8099. https://doi.org/10.1038/s41598-017-08192-7.
Di Maggio, C., Di Trapani, F.P., Madonia, G., Salvo, D., Vattano, M., 2009. First report on the sinkhole phenomena in the Sicilian evaporites (Southern Italy). In: In Abstract volume "I Sinkholes. Gli sprofondamenti catastrofici nell'ambiente naturale ed in quello antropizzato - Sinkholes. The catastrophic sinking in natural and anthropic environments", ISPRA-SGI, December 2-3, 2009. Rome, Italy, p. 40.
Dia, A.N., Castrec-Rouelle, M., Boulege, J., Comeau, P., 1999. Trinidad mud volcanoes where do the expelled fluids come from? Geochim. Cosmochim. Acta 63, 1023–1038.
Doglioni, C., Innocenti, F, Mariotti, S., 2001. Why Mt. Etna? Terra Nova 13, 25–31.
Drago, A., 2005. Atlante climatologico della Sicilia. Seconda edizione. Rivista Italiana di Agrometeorologia 2, 67–83.
Dunai, T.J., Baur, H., 1995. Helium, neon, and argon systematics of the European subcontinental mantle: implications for its geochemical evolution. Geochim. Cosmochim. Acta 59, 2767–2783.
Etiope, G., Caracausi, A., Favara, R., Italiano, F., Baciu, C., 2002. Methane emission from the mud volcanoes of Sicily (Italy). Geophys. Res. Letters 29, 1215. https://doi.org/10.1029/2001GL014340.
Etiope, G., Feyzullayev, A., Milkov, A.V., Waseda, A., Mizobe, K., Sun, C.H., 2009. Evidence of subsurface anaerobic biodegradation of hydrocarbons and potential secondary methanogenesis in terrestrial mud volcanoes. Mar. Petrol. Geol. 26, 1692–1703.
Fancelli, R., Nuti, S., Taffi, L., Monteleone, S., Pipitone, G., 1994. Studio idrogeochimico e termico per la valutazione della Sicilia occidentale. Inventario delle Risorse Geotermiche Nazionali. Ministero dell'industria, del commercio e dell'artigianato. CNR-Istituto Internazionale per le Ricerche Geotermiche, Pisa.
Favara, R., Grassa, F., Inguaggiato, S., D'Amore, F., 1998. Geochemical and hydrogeological characterization of thermal springs in Western Sicily. Italy. Journal of Volcanology and Geothermal Research 84 (1–2).
Favara, R., Grassa, F., Inguaggiato, S., Valenza, M., 2001. Hydrogeochemistry and stable isotopes of thermal springs: earthquake-related chemical changes along Belice Fault (Western Sicily). Appl. Geochem. 16, 1–17.
Frondini, F., 2008. Geochemistry of regional aquifer systems hosted by carbonate-evaporite formations in Umbria and southern Tuscany (central Italy). Appl. Geochem. 23, 2091–2104.
Gasparini, P., Iannaccone, G., Scandone, P., Scarpa, R., 1982. Seismotectonics of the Calabrian Arc. Tectonophysics 84, 267–286.
Gautheron, C., Moreira, M., Allegre, C., 2005. He, Ne and Ar composition of the European lithospheric mantle. Chem. Geol. 217, 97–112.
Gemmellaro, C., 1831. Relazione dei fenomeni del nuovo vulcano sorto dal mare fra la costa di Sicilia e l'Isola di Pantelleria nel mese di luglio 1831, 48. ne' torchi della Regia Università Carmelo Pastore, Catania, p. 25.
Giammanco, S., Palano, M., Scaltrito, A., Scarfì, L., Sortino, F., 2008. Possible role of fluid overpressure in the generation of earthquake swarms in active tectonic areas: The case of the Peloritani Mts. (Sicily, Italy). J. Volcanol. Geotherm. Res. 178, 795–806.
Gianelli, G., Grassi, S., 2001. Water–rock interaction in the active geothermal system of Pantelleria. Italy. Chem. Geol. 181, 113–130.
Giggenbach, W.F., Sano, Y., Wakita, H., 1993. Isotopic composition of helium, and CO_2 and CH_4 contents in gases produced along the New Zealand part of a convergent plate boundary. Geochim. Cosmochim. Acta 57, 3427–3455.
Giggenbach, W.F., 1988. Geothermal solute equilibria. Derivation of Na-K-Mg-Ca geoindicators. Geochim. Cosmochim. Acta 52, 2749–2765.
Giggenbach, W.F., 1991. Chemical techniques in geothermal exploration. In: D'Amore, F. (Ed.), Application of Geochemistry in Geothermal Reservoir Development. UNITAR Publish, Rome, Italy, pp. 119–144.
Giggenbach, WF, Gonfantini, R, Jangi, BL, Truesdell, AH., 1983. Isotopic and chemical composition of Parbati Valley geothermal discharges. NW-Himalaya, India. Geothermics. 12, 199–222.
Grassa, F., Capasso, G., Favara, R., Inguaggiato, S., 2004. Molecular and isotopic composition of free hydrocarbon gases from Sicily. Italy Geophysical Research Letters 31, L06607. https://doi.org/10.1029/2003GL019362.
Grassa, F., Capasso, G., Favara, R., Inguaggiato, S., 2006. Chemical and Isotopic Composition of Waters and Dissolved Gases in Some Thermal Springs of Sicily and Adjacent Volcanic Islands. Italy. Pure Appl. Geophys. 163, 781–807.
Guo, Q., Liu, M., Li, J., Zhang, X., Guo, W., Wang, Y., 2017. Fluid geochemical constraints on the heat source and reservoir temperature of the Banglazhang hydrothermal system, Yunnan-Tibet Geothermal Province. China. J. Geochem. Expl. 172, 109–119.
Heller, C., 2011. Fluid venting structures of terrestrial mud volcanoes (Italy) and marine cold seeps (Black Sea) - Organo-geochemical and biological approaches. PhD Thesis. University of Göttingen, Germany.

Hooker, P.J., Bertrand, R., Lombardi, S., O'Nions, R.K., Oxburgh, E.R., 1985. Helium-3 anomalies and crust-mantle interaction in Italy. Geochim. Cosmochim. Acta 49, 2505–2513.
Italiano, F., Bonfanti, P., Caracausi, A., Ditta, M., Favara, R., Gagliano Candela, E., Maugeri, R., Nigro, F., Renda, P., Scaletta, C., 2006. Attività di emissione di fluidi lungo strutture tettoniche: risultati nell'area della Sicilia Nord-Orientale. GNGTS 302–305. November 28-30, 2006 (Rome, Italy), Abstract book.
Langelier, W., Ludwig, H., 1942. Graphical methods for indicating the mineral character of natural waters. J. Am. Water Assoc. 34, 335–352.
Liotta, M., Grassa, F., D'Alessandro, W., Favara, R., Gagliano Candela, E., Pisciotta, A., Scaletta, C., 2013. Isotopic composition of precipitation and groundwater in Sicily. Italy. Appl. Geoch. 34, 199–206.
Madonia, P., Grassa, F., Cangemi, M., Musumeci, C., 2011. Geomorphological and geochemical characterization of the 11 August 2008 mud volcano eruption at S. Barbara village (Sicily, Italy) and its possible relationship with seismic activity. Nat. Haz Earth Sys. Sci. 11, 1545–1557.
Marty, B., Jambon, A., 1987. C/3He in volatile fluxes from the solid Earth: implications for carbon geodynamics. Earth Planet. Sci. Lett. 83, 16–26.
Messina, A., Lentini, F., Macaione, E., Carbone, S., Doherty, A., 2013. Tectono-stratigraphic evolution of the Southern sector of the Calabria-Peloritani Chain: state of knowledge. Italian Geological Survey and Italian Society of Geology. Geol. F. Trips 5 (2.2), 163. https://doi.org/10.3301/GFT.2013.04.
Minissale, A., 2004. Origin, transport and discharge of CO2 in central Italy. Earth Sci. Rev. 66, 89–141.
Minissale, A., Evans, W.C., Magro, G., Vaselli, O., 1997b. Multiple source components in gas manifestations from north-central Italy. Chem. Geol. 142, 175–192.
Minissale, A., Magro, G., Martinelli, Vaselli O., Tassi, F., 2000. Fluid geochemical transect in the Northern Apennines (central-northern Italy): fluid genesis and migration and tectonic implications. Tectonophysics 319, 199–222.
Minissale, A., Vaselli, O., 2011. Karst springs as "natural" pluviometers: Constraints on the isotopic composition of rainfall in the Apennines of central Italy. Appl. Geochem. 26, 838–852.
Minissale, A., Donato, A., Procesi, M., Pizzino, L., Giammanco, S., 2019. Systematic review of geochemical data from thermal springs, gas vents and fumaroles of Southern Italy for geothermal favourability mapping. Earth-Science Reviews 188 (January 2019), 514–535.
Monaco, C., Mazzoli, S., Tortorici, L., 1996. Active thrust tectonics in Western Sicily (southern Italy): the 1968 Belice earthquake sequence. Terra Nova 8, 372–381.
Montanari, D., Albanese, C., Catalano, R., Contino, A., Fedi, M., Gola, G., Iorio, M., La Manna, M., Monteleone, S., Trumpy, E., Valenti, V., Manzella, A., 2014. Contourmap of the top of the regional geothermal reservoir of Sicily (Italy). J. Maps. https://doi.org/10.1080/17445647.2014.935503.
Montanari, D., Minissale, A., Doveri, M., Gola, G., Trumpy, E., Santilano, A., Manzella, A., 2017. Geothermal resources within carbonate reservoirs in western Sicily (Italy): A review. Earth Sci. Rev. 169, 180–201.
Murray, J.W., Grundmanis, V., Smethie, W.M., 1978. Interstitial water chemistry in the sediments of Saanich inlet. Geochim. Cosmochim. Acta 42, 1011–1026.
Nigro, F., Renda, P., 1999. The north central-Sicily belt: structural setting and geological evolution. Ann. Soc. Geolog. Pol 69, 49–61.
O'Nions, R., Oxburgh, E., 1988. Helium, volatile fluxes and the development of continental crust. Earth Planet. Sci. Lett. 90, 331–347.
Ogniben, L., 1960. Note illustrative dello schema geologico della Sicilia nord-orientale, 64-65. Rivista Mineral. Sicil, pp. 183–212. In Italian with English abstract.
Pallasser, R.J., 2000. Recognising biodegradation in gas/oil accumulations through the δ13C compositions of gas components. Org. Geochem. 31, 1363–1373.
Parkhurst, D., Appelo, D.L., 1999. User's guide to PHREEQC (version 2): a computer program for speciation batch-reaction, one-dimensional transport and inverse geochemical calculations. USGS Water Resources Investigations. Denver, CO (USA), p. 309pp. Report 99 - 4259.
Peccerillo, A., 2017. The Sicily Province. In: Cenozoic Volcanism in the Tyrrhenian Sea Region. Advances in Volcanology. Springer, Cham, pp. 265–312.
Poreda R. J., Craig H., Arnórsson S., Welhan J. A., 1992. Helium isotopes in Icelandic geothermal systems: I. 3He, gas chemistry, and 13C relations.
Regione Siciliana, Piano di Tutela delle Acque della Regione Sicilia, 2006. Prima caratterizzazione e monitoraggio delle Acque Sotterranee finalizzata alla redazione del "Piano di Tutela delle Acque della Regione Sicilia. Commissario Delegato per l'Emergenza Rifiuti e Tutela delle Acque.
Rizzo, A., Barberi, F., Carapezza, M.L., Di Piazza, A., Francalanci, L., Sortino, F., D'Alessandro, W., 2015. New mafic magma refilling a quiescent volcano: evidence from He-Ne-Ar isotopes during the 2011–2012 unrest at Santorini. Greece. Geochem. Geophys. Geosyst. 16, 798–814.
Roure, F., Howell, D.G., Muller, C., Moretti, I., 1990. Late Cenozoic subduction complex of Sicily. J. Struct. Geol 2, 259–266.
Sano, Y., Marty, B., 1995. Origin of carbon in fumarolic gas from island arcs. Chem. Geol. 119 (1-4), 263–274.
Sano, Y., Wakita, H., 1985. Geographical Distribution of $^{3}He/^{4}He$ Ratios in Japan Implications for Arc Tectonics and Incipient Magmatism. J. Geophys. Res. 90 (b10), 8729–8741.
Shimizu, A., Sumino, H., Nagao, K., Notsu, K., Mitropoulos, P., 2005. Variation in noble gas isotopic composition of gas samples from the Aegean arc. Greece. J. Volcanol. Geotherm. Res. 140, 321–339. https://doi.org/10.1016/j.jvolgeores.2004.08.016.
Tassi, F., Bonini, M., Montegrossi, G., Capecchiacci, F., Capaccioni, B., Vaselli, O., 2012a. Origin of light hydrocarbons in gases from mud volcanoes and CH_4-rich emissions. Chem. Geol. 294–295, 113–126.
Tassi, F., Fiebig, J., Vaselli, O., Nocentini, M., 2012b. Origins of methane discharging from volcanic, hydrothermal and cold emissions in Italy. Chem. Geol. 310-311, 36–48.
Tassi, F, Vaselli, O, Luchetti, G, Montegrossi, G, Minissale, A, 2008. [Metodo per la determinazione dei gas disciolti in acque naturali], p. 1-12.[Article in Italian]. Int. Rep. CNRIGG Florence no 10450-11.
Tassi, F., Montegrossi, G., Vaselli, O., Liccioli, C., 2009. Degradation of C2-C15 volatile organic compounds in a landfill cover soil. Science of the Total Environment 407, 4513–4525.
Torfstein, A., Hammerschmidt, K., Friedrichsen, H., Starinsky, A., Garfunkel, Z., Kolodny, Y., 2013. Helium isotopes in Dead Sea transform waters. Chem. Geol. 352, 188–201.
Trabelsi, R., Abid, K., Zouari, K., Yahyaoui, H., 2012. Groundwater salinization processes in shallow coastal aquifer of Djeffara plain of Medenine. Southeastern Tunisia. Environ. Earth Sci. 66, 641–653.
Truesdell A.H., Hulston J.R., 1980. Isotopic evidence on environments of geothermal systems. In: Fritz, P., Fontes, J.Ch. (Eds.), Handbook of Environmental Isotope Geochemistry. The Terrestrial Environment, A, vol. 1. Elsevier, 179–226.
Trumpy, E., Donato, A., Gianelli, G., Gola, G., Minissale, A., Montanari, D., Santilano, A., Manzella, A., 2015. Data integration and favourability maps for exploring geothermal systems in Sicily, southern Italy. Geothermics 56, 1–16.
Vaselli, O., Tassi, F., Montegrossi, G., Capaccioni, B., Giannini, L., 2006. Sampling and analysis of fumarolic gases. Acta Vulcanol 1-2, 65–76.
Venturi, S., Tassia, F., Magib, F., Cabassia, J., Ricci, A., Capecchiacci, F., Caponi, C., Nisi, B., Vaselli, O., 2019. Carbon isotopic signature of interstitial soil gases reveals the potential role of ecosystems in mitigating geogenic greenhouse gas emissions: Case studies from hydrothermal systems in Italy. Science of The Total Environment Volume 655, 887–898.
You, C.F., Gieskes, J.M., Lee, T., Yui, T.F., Chen, H.W., 2004. Geochemistry of mud volcano fluids in the Taiwan accretionary prism. Appl. Geochem. 19, 695–707.
Yuce, G., Italiano, F., D'Alessandro, W., Yalcin, T.H., Yasind, D.U., Gulbay, A.H., Ozyurt, N.N., Rojay, B., Karabacak, V., Bellomo, S., Brusca, L., Yang, T., Fug, C.C., Lai, C.W., Ozacar, A., Walia, V., 2014. Origin and interactions of fluids circulating over the Amik Basin (Hatay, Turkey) and relationships with the hydrologic, geologic and tectonic settings. Chem. Geol. 388, 23–39.
Washington, H.S., 1909. The submarine eruption of 1831 and 1891 near Pantelleria. Am. J. Sci. 27, 131–150. https://doi.org/10.2475/ajs.s4-27.158.131.
Zaidi, F.K., Nazzal, Y., Jafri, M.K., Naeem, M., Ahmed, I., 2015. Reverse ion exchange as a major process controlling the groundwater chemistry in an arid environment: a case study from northwestern Saudi Arabia. Environ Monit Assess 187, 607. https://doi.org/10.1007/s10661-015-4828-4, 2015.